SAMSO TR 74-88

SURFACE SCATTER STUDY

Roland V. Shack
Michael A. DeBell

Optical Sciences Center
The University of Arizona
Tucson, Arizona 85721

February 1974

Final Report for Period March 1972 to January 1973

Approved for public release; distribution unlimited.

Prepared for the
Space and Missile Systems Organization
Air Force Systems Command
Los Angeles Air Force Station, California

AVAILABILITY NOTICE

Approved for public release; distribution unlimited.

Copies of this report may be obtained from the Defense Documentation Center, Cameron Station, Alexandria, Virginia 22314.

DISPOSITION INSTRUCTIONS

Do not return this copy. Retain or destroy.

REPRODUCTION NOTICE

This report may be reproduced for any purpose of the U. S. Government.

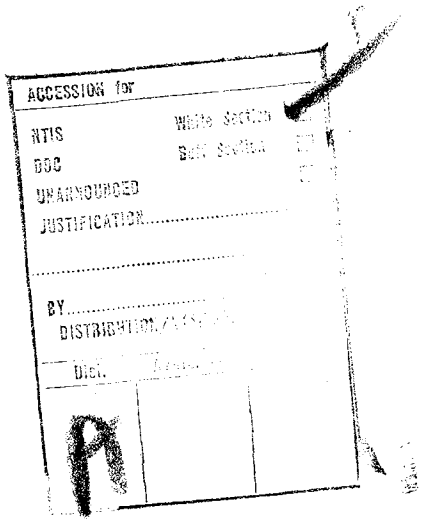

UNCLASSIFIED

SECURITY CLASSIFICATION OF THIS PAGE *(When Data Entered)*

REPORT DOCUMENTATION PAGE		READ INSTRUCTIONS BEFORE COMPLETING FORM
1. REPORT NUMBER SAMSO TR 74-88	2. GOVT ACCESSION NO.	3. RECIPIENT'S CATALOG NUMBER
4. TITLE *(and Subtitle)* SURFACE SCATTER STUDY		5. TYPE OF REPORT & PERIOD COVERED Final Report for Period March 1972 to January 1973
		6. PERFORMING ORG. REPORT NUMBER
7. AUTHOR(s) Roland V. Shack Michael A. DeBell		8. CONTRACT OR GRANT NUMBER(s) F04701-72-C-0181
9. PERFORMING ORGANIZATION NAME AND ADDRESS Optical Sciences Center University of Arizona Tucson, Arizona 85721		10. PROGRAM ELEMENT, PROJECT, TASK AREA & WORK UNIT NUMBERS
11. CONTROLLING OFFICE NAME AND ADDRESS SAMSO Air Force Systems Command Los Angeles Air Force Station, California		12. REPORT DATE February 1974 13. NUMBER OF PAGES 76
14. MONITORING AGENCY NAME & ADDRESS *(if different from Controlling Office)*		15. SECURITY CLASS. *(of this report)* Unclassified 15a. DECLASSIFICATION/DOWNGRADING SCHEDULE

16. DISTRIBUTION STATEMENT *(of this Report)*

Approved for public release; distribution unlimited.

17. DISTRIBUTION STATEMENT *(of the abstract entered in Block 20, if different from Report)*

18. SUPPLEMENTARY NOTES

19. KEY WORDS *(Continue on reverse side if necessary and identify by block number)*

Surface Properties
Optical Surfaces
Scattered Light
Diffraction Theory
Diffuse Reflectance

20. ABSTRACT *(Continue on reverse side if necessary and identify by block number)*

The angular spectrum of plane waves approach to scalar diffraction theory has been extended to include scattering. An instrument was designed and constructed to measure scattered light distributions from aluminized glass surfaces. Diffuse reflectance measurements were made on samples having varying degrees of surface finish. Results of these measurements as a function of angle of incidence and wavelength are reported.

DD FORM 1 JAN 73 1473 EDITION OF 1 NOV 65 IS OBSOLETE
S/N 0102-014-6601

UNCLASSIFIED

SECURITY CLASSIFICATION OF THIS PAGE *(When Data Entered)*

FOREWORD

This is the final report for the surface scatter study program undertaken by the Optical Sciences Center, University of Arizona, Tucson, Arizona. The work was performed under Air Force Contract F04701-72-C-0181. The program was carried out under the auspices of the Air Force Space and Missile Systems Organization.

The principal investigator for the Optical Sciences Center was Roland V. Shack. The project engineer and co-investigator was Michael A. DeBell.

SUMMARY

Scattering theory is developed as an extension of the angular spectrum of plane waves approach to diffraction. Expressions useful in the evaluation of scatter are obtained through the introduction of random perturbations in the pupil function. When the surface statistics are known the expected value of the transfer function can be found. The particular case of a surface with Gaussian statistics is then treated and expressions are derived that predict the scattered flux distribution for a surface with such statistics.

Apparatus is described that is capable of measuring the scattered flux distribution in the range of two to ninety degrees from the specular direction. Using this apparatus the distribution of light scattered by a variety of plane mirror surfaces as a function of roughness, angle of incidence, and wavelength is measured experimentally.

The intensity of the scattered light is shown to vary with the inverse square of the wavelength when the total scattered flux is small compared to the specularly reflected flux. This theory is consistent with the data.

A numerical integration of the scattered light distribution yields the total scattered flux. A relationship between the total scattered flux and the surface roughness is derived. The theoretical results and the estimated roughness were found to be of the same order of magnitude.

TABLE OF CONTENTS

LIST OF ILLUSTRATIONS

LIST OF TABLES

I

INTRODUCTION

When light is incident upon a surface the reflected flux can be described by considering two components, the specular component and the diffuse component. The specular component is reflected in the plane of incidence at an angle equal to the angle of incidence and is coherent with the incident beam. Light scattered away from the specular direction is said to be diffusely reflected. Diffusely reflected light is a diffraction phenomena and its distribution is attributable to the surface properties of the reflector. Properties that can be used to characterize such surfaces are roughness, autocorrelation length, and the statistical distributions of these two parameters.

Two special cases are of interest: the perfect reflector and the perfectly diffuse, or Lambertian, reflector. A perfect reflector alters the direction and not the distribution of the incident light. A plane surface that is perfectly diffuse obeys Lambert's cosine law, $I(\theta) = I_o \cos\theta$, where $I(\theta)$ is the radiant intensity at an angle θ to the surface and I_o is the radiant intensity measured normal to the surface. Theories put forth should reduce to these special cases in the limit and it is in this regard that we mention them.

Previous Theoretical Work

Scattering from surfaces is a diffraction phenomena and as such has been treated as a boundary value problem where Maxwell's equations are applied. Two categories exist in this general body of theory: that in which scattering is treated for a specific model of the surface and that in which the surface is statistically described by a distribution of heights and slopes about a mean surface.

Examples of theoretical approaches, for a specific surface model, have been proposed by Beckman and Spizzichino (1963), Berreman (1967), Hunderi and Beaglehole (1970), and Twersky (1957). Twersky and Berreman have considered surface models for which it is possible to obtain exact solutions for the electromagnetic field. In these cases the Kirchhoff approximations are applied to the boundary conditions in order to evaluate the Helmholtz integral. Their models consist of randomly distributed hemispherical irregularities on an otherwise smooth surface. Twersky arrived at complete solutions by considering only perfect conductors while Berreman made first-order calculations applicable to surfaces of any conductivity. Hunderi and Beaglehole adopted an approach that yields the reflectance of a surface model consisting of spheres located just above a smooth metal surface. Although this model of a scattering surface is not as realistic as that of Berreman, it can be solved exactly for a metal with any conductivity.

Theory relating to periodically rough surfaces is discussed by Beckmann and Spizzichino. They use the Kirchhoff method of approximating the boundary conditions on a perfectly conducting periodic surface and then find the

corresponding field by using the Helmholtz integral. Making additional approximations they deal with the surfaces that are not perfect conductors.

Perhaps the best known theory dealing with statistical scatter from surfaces having roughness distributions is that of Davies (1954). His theory considers only the phase modulation of the incident light by the height variations along the surface. The specular and scattered light are found by summing the radiation from Huygens wavelets at the surface. The height variation is then assumed to be normally distributed about its mean with an rms deviation of σ. The scattering theory then predicts that the ratio of the specular reflectivity of a rough surface to that of a smooth surface varies as

$$R/R_o = e^{-(4\pi\sigma/\lambda)^2}$$

and makes similar predictions about the angular distribution of scattered light. The approximations made in this development limit the theory so that it is valid only if the typical distance separating surface structures is on the order of a wavelength or larger. This theory of Davies was extended by Bennett and Porteus (1961) and by Porteus (1963). Work by Beckmann and Spizzichino (1963) also extended the statistical approach of Davies.

Previous Experimental Investigations

Lord Rayleigh (1901) was one of the earliest investigators of scattered light. He noted the effect of poorly polished surfaces on optical performance. His work examined the effects caused by surface roughness, wavelength, and angle of incidence on the reflected beam. The variation in brightness with angle of observation for various surfaces was studied by Jones (1922). He used what he termed a "goniophotometer"; a device having means of directing a collimated beam on a sample surface and a photometer arm arranged to measure the brightness of the surface. The angle of illumination could be varied and the angle of viewing held constant or vice versa. Slater (1935) improved on this goniophotometer and was able to provide quantitized measurements in either transmission or reflection.

Photometric measurements by Hunter (1940) employed a barrier layer photocell to measure the diffuse reflectance of a broad range of samples. His work included a detailed report on sources of error. Hunter used aluminized "perfect mirrors" as reference standards. Some of the first work where scattering itself was a primary concern was reported by Aughey and Baum (1954). The scattering profiles they measured led them to direct conclusions about the physical properties of the scatterer.

The scattering theory of Davies (1954) was expanded and experimentally investigated by Bennett and Porteus (1961). From this work and work that followed shortly thereafter (Bennett, 1963 and Porteus, 1963) the reflectance properties of samples with a measured surface roughness were directly compared to theory. In their work Bennett and Porteus reported good agreement between the measurements on their samples and the theory they had

developed. The thrust of these measurements led to investigations at the Optical Sciences Center by D. McKenney, L. Mott, G. Orme and M. DeBell.

Semplak (1965) and Blazey (1967) along with others (see annotated bibliography) used lasers as a light source for their scattering measurements. Blazey, using a goniometric scanning device reported results in good agreement with the Beckmann theory. His measurements were made on multi-layer dielectric coatings typical of those used in the laser industry.

Orme (1972), using a clever diffraction technique, was able to explore the zeros of a single slit diffraction pattern and evaluate scatter to within one-third of a degree of the specular beam. Orme made wide angle measurements using a goniometric device. Using this technique he was able to explore all but the limited region of, 1.5° to 5°, from the specular direction, in the plane of incidence. His work, as had the work of Aughey and Baum, pointed to the possibility that scatter was caused by two different mechanisms. The inability of Orme to make measurements in the 1.5° to 5° range and the questions raised concerning multiple scattering phenomena have provided the stimulation to undertake the work reported here.

II

THEORY

The Angular Spectrum of Plane Waves Approach to Diffraction Theory

The aim of this section is to cast diffraction theory in a format that will make it useful in examining the effects of scattering. We will distinguish scatter from diffraction by defining scatter as "diffraction from a surface or medium whose properties are statistical in nature." Our approach will be to consider a disturbance in an initial plane, P_1, and to derive the necessary theory that will allow us to predict the field in a subsequent plane, P_2.

Let the complex amplitude distribution at the plane P_1 be $U(x,y,0)$ and consider the geometry shown in Fig. 1 below. The scalar disturbance on P_1

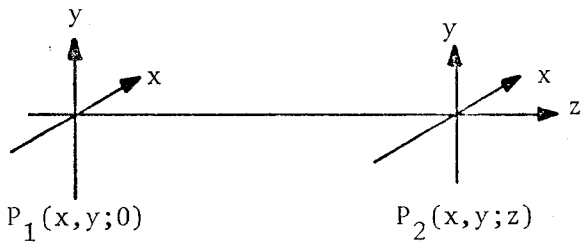

Fig. 1. Geometry of planes P_1 and P_2.

will be considered the only radiation contributing to the field at P_2. It will be assumed that the light propagating from P_1 to P_2 obeys the Helmholtz equation. Further we will assume that the Fourier transform of the scalar field $U(x,y,0)$ exists. (We can make this assumption since as Goodman points out, "physical possibility is a valid and sufficient condition for the existence of a transform.")

We can now define the Fourier transform relationships that exist for planes P_1 and P_2.

$$A_o(\xi,\eta;0)^{\dagger} = \iint_{-\infty}^{\infty} U_o(x,y;0)\ e^{-i2\pi(x\xi + y\eta)}\,dxdy \tag{1}$$

$$A(\xi,\eta;z) = \iint_{-\infty}^{\infty} U(x,y;z)\ e^{-i2\pi(x\xi + y\eta)}\,dxdy \tag{2}$$

$$U_o(x,y;0) = \iint_{-\infty}^{\infty} A_o(\xi,\eta;0)\ e^{i2\pi(\xi x + \eta y)}\,d\xi d\eta \tag{3}$$

$$U(x,y;z) = \iint_{-\infty}^{\infty} A(\xi,\eta;z)\ e^{i2\pi(\xi x + \eta y)}\,d\xi d\eta. \tag{4}$$

($^{\dagger}z$ has a parametric relationship since it is a function of the observation plane.)

Notice that the integrand in Eqs. (3) and (4) has a form similar to that of a plane wave. The equation for a unit amplitude plane wave is

$$e^{i\vec{k}\cdot\vec{r}}.$$

Here $\vec{k}$ is the propagation vector and $\vec{r}$ is the position vector (see Fig. 2).

$$\vec{k} = \frac{2\pi}{\lambda}(\alpha\bar{x} + \beta\bar{y} + \gamma\bar{z}) \tag{5}$$

$$\vec{r} = x\bar{x} + y\bar{y} + z\bar{z} \tag{6}$$

where

$\bar{x}$, $\bar{y}$ and $\bar{z}$ are unit vectors, and,

α, β and γ are direction cosines

$\alpha^2 + \beta^2 + \gamma^2 = 1.$

The unit amplitude plane wave can then be rewritten as:

$$e^{i\vec{k}\cdot\vec{r}} = e^{i(\alpha x + \beta y + \gamma z)2\pi/\lambda}. \tag{7}$$

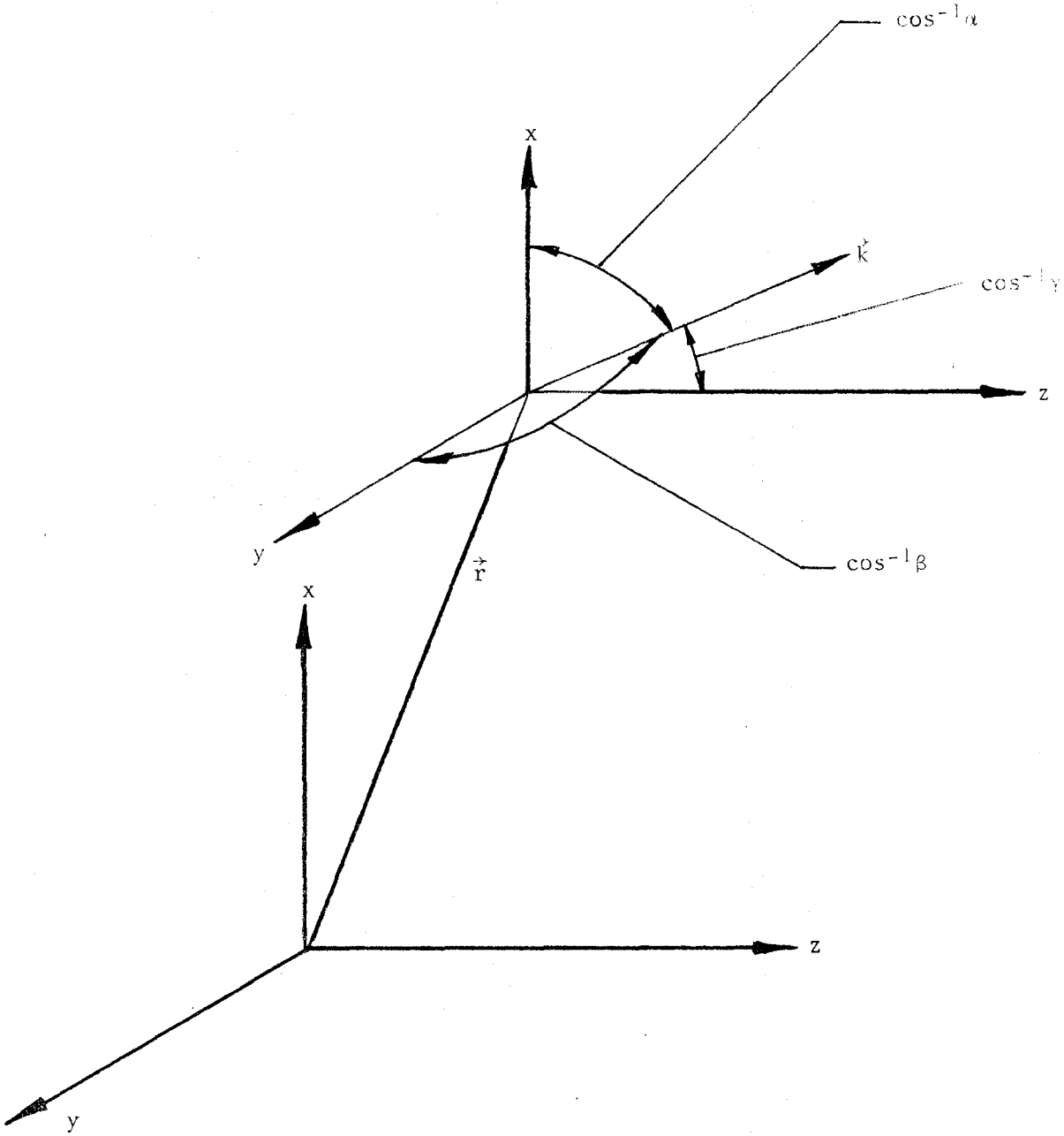

Fig. 2. Relationship of the propagation vector to its direction cosines.

Across the plane z = 0, the integrand of Eq. (3) can be thought of as the intersection of that plane with a plane wave traveling with direction cosines:

$$\alpha = \lambda\xi, \quad \beta = \lambda\eta \quad \text{and} \quad \gamma = \sqrt{1 - (\lambda\xi)^2 - (\lambda\eta)^2}. \tag{8}$$

It now becomes convenient to scale the variables x, y, and z to the wavelength, λ. These new variables are denoted $\hat{x}$, $\hat{y}$, and $\hat{z}$;

$$\hat{x} = \frac{x}{\lambda}; \quad \hat{y} = \frac{y}{\lambda}; \quad \hat{z} = \frac{z}{\lambda}. \tag{9}$$

With this notation, Eqs. (1) - (4) can be rewritten as:

$$A_o(\alpha,\beta;0) = \int_{-\infty}^{\infty}\int U_o(\hat{x},\hat{y};0)\ e^{-i2\pi(\alpha\hat{x} + \beta\hat{y})}d\hat{x}d\hat{y} \tag{10}$$

$$A(\alpha,\beta;\hat{z}) = \int_{-\infty}^{\infty}\int U(\hat{x},\hat{y};\hat{z})\ e^{-i2\pi(\alpha\hat{x} + \beta\hat{y})}d\hat{x}d\hat{y} \tag{11}$$

$$U_o(\hat{x},\hat{y};0) = \int_{-\infty}^{\infty}\int A_o(\alpha,\beta;0)\ e^{i2\pi(\alpha\hat{x} + \beta\hat{y})}d\alpha d\beta \tag{12}$$

$$U(\hat{x},\hat{y};\hat{z}) = \int_{-\infty}^{\infty}\int A(\alpha,\beta;\hat{z})\ e^{i2\pi(\alpha\hat{x} + \beta\hat{y})}d\alpha d\beta. \tag{13}$$

Here we have cast the integrand into the form of plane waves modified by Fourier coefficients.

The disturbances in planes P_1 and P_2 must also satisfy the Helmholtz equation:

$$(\nabla^2 + k^2)U = 0. \tag{14}$$

Here,

$$k = 2\pi/\lambda$$

$$\nabla^2 = \frac{\partial^2}{\partial x^2} + \frac{\partial^2}{\partial y^2} + \frac{\partial^2}{\partial z^2} .$$

In the scaled coordinate system, $\hat{\nabla}^2 = \lambda^2\nabla^2$, and $\hat{k}^2 = \lambda^2 k^2 = (2\pi)^2$. With these substitutions, Eq. (14) becomes:

$$(\hat{\nabla}^2 + (2\pi)^2)U = 0. \tag{15}$$

If we apply Eq. (15) to Eq. (13) we get:

$$\int_{-\infty}^{\infty}\int (\hat{\nabla}^2 + (2\pi)^2)A(\alpha,\beta;\hat{z})e^{i2\pi(\alpha\hat{x} + \beta\hat{y})}d\alpha d\beta = 0 \tag{16}$$

or

$$\int_{-\infty}^{\infty}\int \left[\frac{\partial^2}{\partial z^2} A(\alpha,\beta;\hat{z})e^{i2\pi(\alpha\hat{x}+\beta\hat{y})} + A(\alpha,\beta;\hat{z})(i2\pi\alpha)^2 e^{i2\pi(\alpha\hat{x}+\beta\hat{y})}\right.$$

$$+ A(\alpha,\beta;\hat{z})(i2\pi\beta)^2 e^{i2\pi(\alpha\hat{x}+\beta\hat{y})}$$

$$\left. + 2\pi^2 A(\alpha,\beta;\hat{z})e^{i2\pi(\alpha\hat{x}+\beta\hat{y})}\right]d\alpha d\beta = 0 \tag{17}$$

hence,

$$\int_{-\infty}^{\infty}\int \left[\frac{\partial^2}{\partial \hat{z}^2} A(\alpha,\beta;\hat{z}) + 4\pi^2 A(\alpha,\beta;\hat{z})(1-\alpha^2-\beta^2)\right]e^{i2\pi(\alpha\hat{x}+\beta\hat{y})}d\alpha d\beta = 0. \tag{18}$$

The Fourier transform of the function in brackets is zero so the function itself must be identically zero. Thus we can write:

$$\frac{\partial^2}{\partial \hat{z}} A(\alpha,\beta;\hat{z}) + 4\pi^2\gamma^2 A(\alpha,\beta;\hat{z}) = 0, \tag{19}$$

since $\gamma^2 = (1-\alpha^2-\beta^2)$. This equation has a solution of the form:

$$A(\alpha,\beta;\hat{z}) = A_o(\alpha,\beta;0)\ e^{i2\pi\gamma\hat{z}}. \tag{20}$$

Equation (2) then relates the Fourier transforms of the scalar fields in planes P_1 and P_2. Indeed Eq. (20) can be rewritten in terms of a transfer function for free space, H;

$$A(\alpha,\beta;\hat{z}) = A_o(\alpha,\beta;0)H(\alpha,\beta;\hat{z}). \quad H(\alpha,\beta;\hat{z}) = e^{i2\pi\gamma\hat{z}} \tag{21}$$

We have thus far applied no restrictions on γ and two regions of interest are apparent; that for real values of γ and that for imaginary values.

$$\gamma = [1 - (\alpha^2+\beta^2)]^{\frac{1}{2}} \quad \text{for } (\alpha^2 + \beta^2) \leq 1 \quad \gamma \text{ is } \underline{\text{real}}$$

$$\text{for } (\alpha^2 + \beta^2) > 1 \quad \gamma \text{ is } \underline{\text{imaginary}} \tag{22}$$

Where γ is real the various plane wave components of the angular spectrum propagate in different directions and thus reach the "observation point" in plane P_2 with an associated phase factor

$$e^{i2\pi\gamma\hat{z}}.$$

When γ is imaginary the exponential

$$e^{i2\pi\gamma\hat{z}}$$

becomes a damping function of the form $e^{-K\hat{z}}$ where $K = 2\pi\sqrt{(\alpha^2+\beta^2)-1}$. Waves characterized by these values of γ are rapidly attenuated in the $\hat{z}$ direction.

The spread function associated with our transfer function is its Fourier transform.

$$F\left\{e^{i2\pi\gamma\hat{z}}\right\} = \left(i - \frac{1}{2\pi\hat{r}}\right)\left(\frac{e^{i2\pi\hat{r}}}{\hat{r}}\right)\left(\frac{\hat{z}}{\hat{r}}\right) . \tag{23}$$

This spread function can be cast into the form:

$$a(\hat{r})e^{i\phi(\hat{r})} \quad \text{where} \quad \hat{r}^2 = \hat{x}^2 + \hat{y}^2 + \hat{z}^2. \tag{24}$$

The righthand side of Eq. (23) is straightforwardly separated into its real and imaginary components, a + ib;

$$-\left(\frac{\hat{z}}{\hat{r}}\right)\underbrace{\left(\frac{\sin 2\pi\hat{r}}{\hat{r}} + \frac{\cos 2\pi\hat{r}}{2\pi\hat{r}^2}\right)}_{a} + i\left[\left(\frac{\hat{z}}{\hat{r}}\right)\underbrace{\left(\frac{\cos 2\pi\hat{r}}{\hat{r}} - \frac{\sin 2\pi\hat{r}}{2\pi\hat{r}^2}\right)}_{b}\right] . \tag{25}$$

To represent this in phasor form we first recall the graphical representation shown in Fig. 3.

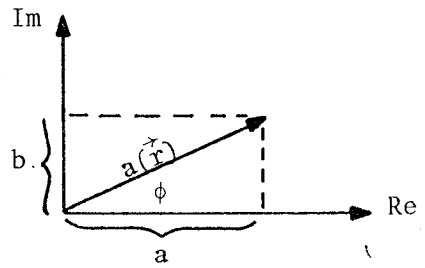

Fig. 3. Phasor representation.

$$a(\hat{r}) = \sqrt{a^2 + b^2} = \frac{\hat{z}}{2\pi\hat{r}^3}\left[1 + (2\pi\hat{r})^2\right]^{\frac{1}{2}} \tag{26}$$

The phase can be expressed as:

$$\phi = \arctan\left(\frac{b}{a}\right) = 2\pi\hat{r} - \arctan\,(2\pi\hat{r}). \tag{27}$$

Hence our spread function can be written as:

$$a(\hat{r})e^{i\phi(\hat{r})} = \frac{\hat{z}}{2\pi\hat{r}^3}\,(1 + (2\pi\hat{r})^2)^{\frac{1}{2}}\, e^{i(2\pi\hat{r} - \tan 2\pi\hat{r})}. \tag{28}$$

The measurements we wish to make have two characteristics that should be considered: measurements are made on a spherical surface and they are made at a distance from the aperture plane that is large compared to the size of the "initial disturbance" and the wavelength of the light that is propagating. Figure 4 shows the geometry that we wish to consider.

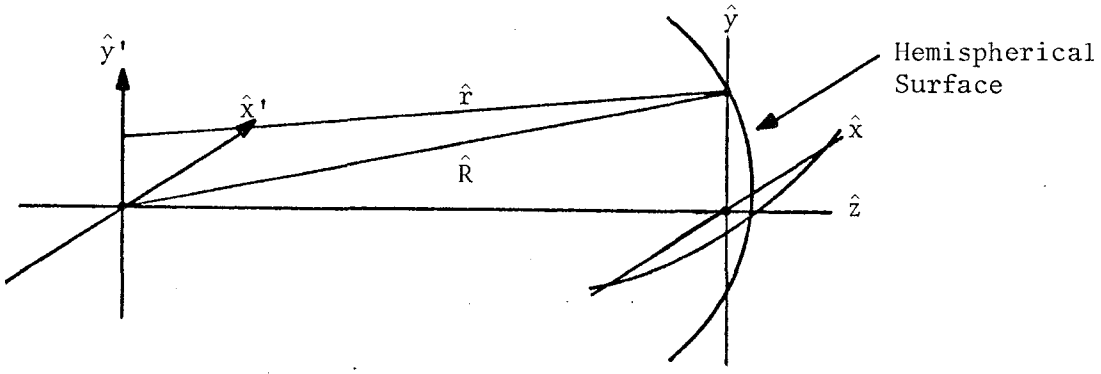

Fig. 4. Relationship of diffraction plane to observation surface.

The primed (') plane is the pupil plane and the spherical surface of radius $\hat{R}$ is where we wish to measure the resultant disturbance. In terms of what has been previously discussed we can write:

$$A(\alpha,\beta;\hat{z}) = A_o(\alpha,\beta;0)\, e^{i2\pi\gamma\hat{z}}$$

$$U(\hat{x},\hat{y};\hat{z}) = F\{A(\alpha,\beta;\hat{z}\}$$

and can then conclude,

$$U(\hat{x},\hat{y};\hat{z}) = F\{A_o(\alpha,\beta;0)\, e^{i2\pi\gamma\hat{z}}\}. \tag{29}$$

Now by the convolution theorem we have:

$$U(\hat{x},\hat{y};\hat{z}) = F\{A_o(\alpha,\beta;0)\} * F\{e^{i2\pi\gamma\hat{z}}\}$$

$$= U(\hat{x}',\hat{y}';0) * \left(i - \frac{1}{2\pi\hat{R}}\right)\frac{\hat{z}}{\hat{R}}\ \frac{e^{i2\pi\hat{R}}}{\hat{R}}\ . \tag{30}$$

The convolution integral can then be taken "over" the pupil plane:

$$U(\hat{x},\hat{y};\hat{z}) = \iint_{-\infty}^{\infty} U(\hat{x}',\hat{y}';0)\,(i - \frac{1}{2\pi\hat{r}})\,(\frac{\hat{z}}{\hat{r}})\left(\frac{e^{i2\pi\hat{r}}}{\hat{r}}\right) d\hat{x}'d\hat{y}' \tag{31}$$

where

$$\hat{r} = \sqrt{(\hat{x}-\hat{x}')^2 + (\hat{y}-\hat{y}')^2 + \hat{z}^2}.$$

Now assume that we are many wavelengths away from the pupil plane. The term $1/2\pi\hat{r}$ then becomes insignificant in the integral compared to the other term. Equation 31 can then be approximated by:

$$U(\hat{x},\hat{y};\hat{z}) = i\iint_{-\infty}^{\infty} U(\hat{x}',\hat{y}';0)\,(\frac{\hat{z}}{\hat{r}})\left(\frac{e^{i2\pi\hat{r}}}{\hat{r}}\right) d\hat{x}'d\hat{y}'. \tag{32}$$

Substituting $\hat{R} + (\hat{r}-\hat{R}) = \hat{r}$, Eq. (36) is rewritten as

$$U(\hat{x},\hat{y};\hat{z}) = i\iint_{-\infty}^{\infty} U(\hat{x},\hat{y};0)\left(\frac{\hat{z}}{\hat{R}}\right)\left(\frac{\hat{R}}{\hat{r}}\right)^2\left(\frac{e^{i2\pi\hat{R}}}{\hat{R}}\right) e^{i2\pi(\hat{r}-\hat{R})} d\hat{x}'d\hat{y}'. \tag{33}$$

But

$$\hat{r}-\hat{R} = \frac{\hat{x}'^2 + \hat{y}'^2}{\hat{r} + \hat{R}} - \frac{2\hat{R}}{\hat{r} + \hat{R}}\,(\alpha_o\hat{x}' + \beta_o\hat{y}'),$$

where

$$\alpha_o = \frac{\hat{x}}{\hat{R}} ; \quad \beta_o = \frac{\hat{y}}{\hat{R}} ; \quad \gamma_o = \frac{\hat{z}}{\hat{R}} .$$

Equation (33) can now be expressed in terms of the direction cosines and the radius $\hat{R}$.

$$U(\alpha_o,\beta_o;\hat{R}) = \frac{i\gamma_o e^{i2\pi\hat{R}}}{\hat{R}} \iint_{-\infty}^{\infty} U(\hat{x}',\hat{y}';0) \left(\frac{\hat{R}}{\hat{r}}\right)^2 e^{i2\pi\left(\frac{\hat{x}'^2 + \hat{y}'^2}{\hat{r} + \hat{R}}\right)} \times e^{-i2\pi \frac{2\hat{R}}{\hat{r}+\hat{R}} (\alpha_o\hat{x}' + \beta_o\hat{y}')} dx'dy'. \tag{35}$$

We now make two approximations:

(a) $\hat{R} + \hat{r} = 2\hat{R}\left(1 + \frac{\hat{r} - \hat{R}}{2\hat{R}}\right) \simeq 2R$, since $\frac{\hat{r} - \hat{R}}{\hat{R}} << 1$ and

(b) $\frac{\hat{R}}{\hat{r}} = \frac{\hat{r} + \hat{R}-\hat{r}}{\hat{r}} = 1 + \frac{\hat{R}-\hat{r}}{\hat{r}}$

$$\therefore \left(\frac{\hat{R}}{\hat{r}}\right)^2 = 1 + \frac{2(\hat{R}-\hat{r})}{\hat{r}} + \left(\frac{\hat{R}-\hat{r}}{\hat{r}}\right)^2 \simeq 1,$$

since $\frac{\hat{R}-\hat{r}}{\hat{r}} << 1.$ (36)

When the approximations expressed in Eqs. (36) are substituted into Eq. (35) we have:

$$U(\alpha_o,\beta_o;\hat{R}) \cong \frac{i\gamma_o e^{i2\pi\hat{R}}}{\hat{R}} \iint_{-\infty}^{\infty} U(\hat{x}',\hat{y}';0) e^{i2\pi\left(\frac{\hat{x}'^2 + \hat{y}'^2}{2R}\right)} \times e^{-i2\pi(\alpha_o\hat{x}' + \beta_o\hat{y}')} d\hat{x}'d\hat{y}'. \tag{37}$$

Equation (37) is the classical Fresnel diffraction expression modified by a spherical wave. The further approximation that

$$e^{i2\pi\left(\frac{\hat{x}'^2 + \hat{y}'^2}{2R}\right)}$$

is equal to 1 leads to the result:

$$U(\alpha_o,\beta_o;\hat{R}) \cong \frac{i\gamma_o e^{i2\pi\hat{R}}}{\hat{R}} \iint_{-\infty}^{\infty} U(\hat{x}',\hat{y}';0)e^{-i2\pi(\alpha_o\hat{x}'+\beta_o\hat{y}')}\,d\hat{x}'d\hat{y}'. \tag{38}$$

This is the Fraunhofer pattern as modified by a spherical wave. From Eq. (11) we know that Eq. (38) can be rewritten as:

$$U_o(\alpha_o,\beta_o;\hat{R}) \cong \frac{i\gamma_o e^{i2\pi\hat{R}}}{\hat{R}} A_o(\alpha_o,\beta_o;0). \tag{39}$$

We have a spherical wave modulated by the Fourier transform of the disturbance in the initial plane. Now let

$$U(\hat{x}',\hat{y}') = a_o\tau(\hat{x}',\hat{y}'). \tag{40}$$

From Eqs. (39) and (40) we can write

$$\frac{\hat{R}}{i\gamma_o} e^{-i2\pi\hat{R}}\, U(\alpha_o,\beta_o,\hat{R}) = A(\alpha_o,\beta_o) = a_o \iint_{-\infty}^{\infty} \tau(\hat{x}',\hat{y}')e^{-i2\pi(\alpha_o\hat{x}'+\beta_o\hat{y}')}\,d\hat{x}'d\hat{y}'. \tag{41}$$

The power theorem will give us the total flux, Φ, viz.,

$$\iint_{-\infty}^{\infty} \frac{\hat{R}^2}{\gamma_o^2} |U(\alpha_o,\beta_o,\hat{R})|^2\, d\alpha_o d\beta_o = a_o^2 \iint_{-\infty}^{\infty} |\tau(\hat{x}',\hat{y}')|^2\, d\hat{x}'d\hat{y}' = \Phi. \tag{42}$$

Noting that $d\omega = d\alpha_o d\beta_o/\gamma_o$, Eq. (42) can be rewritten as:

$$\iint_{\Omega} \frac{\hat{R}^2}{\gamma_o} |U(\alpha_o,\beta_o,\hat{R})|^2 \, d\omega = \frac{a_o{}^2 a}{\lambda^2} = \Phi = \text{total power.} \tag{43}$$

The radiant intensity, I(w/sr), is then

$$I(\alpha_o,\beta_o) = \frac{d\Phi}{d\omega} = \frac{\hat{R}^2}{\gamma_o} |U(\alpha_o,\beta_o,\hat{R})|^2 = \gamma_o |A(\alpha_o,\beta_o)|^2. \tag{44}$$

We note that the radiant intensity is directly proportional to γ and thus we have a cosine dependence.

Scattering Theory

In general the pupil function will include random perturbations that will lead to scatter. In order to treat these perturbations we consider the transfer function V, which is the Fourier transform of the spread function, i.e., $|A|^2 \leftrightarrow V$. The autocorrelation theorem allows us to write the transfer function as in Eq. (45) below.

$$V(\hat{\xi}',\hat{\eta}') = \iint_{-\infty}^{\infty} U(\hat{x}' + \frac{\hat{\xi}'}{z}, \hat{y}' + \frac{\hat{\eta}'}{z}) \times U^*(\hat{x}' - \frac{\hat{\xi}'}{z}, \hat{y}' - \frac{\hat{\eta}'}{z}) d\hat{x}' d\hat{y}' \tag{45}$$

$$= a_o{}^2 \iint_{-\infty}^{\infty} \tau(\hat{x}' + \frac{\hat{\xi}'}{z}, \hat{y}' + \frac{\hat{\eta}'}{z}) \times \tau^*(\hat{x}' - \frac{\hat{\xi}'}{z}, \hat{y}' - \frac{\hat{\eta}'^2}{z}) d\hat{x}' d\hat{y}'. \tag{46}$$

If we assume that the pupil function has random phase variations and no amplitude variations (such as a mirror in the pupil would introduce) we can write τ as:

$$\tau = |\tau| e^{i2\pi(\hat{W}_o + \hat{W}_R)}, \tag{47}$$

where $\hat{W}_R$ indicates the random component. Further, if we introduce the notation:

$$W(+) = W\left(x + \frac{\hat{\xi}'}{z}, y + \frac{\hat{\eta}'}{z}\right)$$

and

$$W(-) = W\left(x - \frac{\hat{\xi}'}{z}, y - \frac{\hat{\eta}'}{z}\right), \tag{48}$$

and take the average, we obtain

$$\langle V(\xi',\eta')\rangle = a_o^2 \iint_{-\infty}^{\infty} |\tau(+)||\tau(-)| e^{i2\pi(\hat{W}_o(+) - \hat{W}_o(-))} \times \left\langle e^{i2\pi(\hat{W}_R(+) - \hat{W}_R(-))} \right\rangle d\hat{x}'d\hat{y}'. \tag{49}$$

The term,

$$\left\langle e^{i2\pi(\hat{W}_R(+) - \hat{W}_R(-))} \right\rangle$$

in Eq. (49) is the only term of the equation that is random. For stationary processes, such as those which describe mirror surfaces, this term is not a function of x' or y' and may thus be taken outside of the integral.

$$\langle V(\hat{\xi}',\hat{\eta}') = e^{i2\pi(\hat{W}_R(+) - \hat{W}_R(-)\rangle} a_o^2 \iint_{-\infty}^{\infty} |\tau(+)||\tau(-)| \times e^{i2\pi(\hat{W}_o(+) - \hat{W}_o(-))} d\hat{x}'d\hat{y}' \tag{50}$$

The expected value of the transfer function may be written as:

$$\left\langle V(\hat{\xi}',\hat{\eta}') \right\rangle = \left\langle e^{i2\pi(\hat{W}_R(+) - \hat{W}_R(-))} \right\rangle V_o. \tag{51}$$

Here V_o can be thought of as a transfer function for a surface without irregularities and the expected value of the term containing the random components as a transfer function for the irregularities. It remains to

determine the form of this expected value. Let us assume a normal distribution for $W_R(+) - W_R(-)$. From random variable theory we find that the expected value for two, real valued, stationary, jointly normal, random processes X(+) and Y(+) is given by:

$$\left\langle e^{X(+)} + e^{iY(+)} \right\rangle = e^{[\eta_x + i\eta_y + \frac{1}{2}(\mu_{20} + iZ\mu_{11} - \mu_{02})]}, \qquad (52)$$

where

$$\eta_x = \langle X(+) \rangle$$

$$\eta_y = \langle Y(+) \rangle \quad \text{and}$$

$$\mu_{jk} = \left\langle (X-\eta_x)^j (Y-\eta_y)^k \right\rangle .$$

In our case, X = 0 and $H(+) = 2\pi(\hat{W}(+) - \hat{W}(-))$ and:

$$\eta_x = \langle X(+) \rangle = 0$$

$$\mu_{20} = 0$$

$$\mu_{11} = 0.$$

$$\langle e^{iY(+)} \rangle = \left\langle e^{i2\pi(\hat{W}_R(+) - \hat{W}_R(-))} \right\rangle = e^{i\eta_y - \frac{1}{2}\mu_{02}}. \qquad (53)$$

For our problem,

$$\eta_y = \langle 2\pi(\hat{W}(+) - \hat{W}(-)) \rangle = \langle 2\pi\hat{W}(+) \rangle - \langle 2\pi\hat{W}(-) \rangle = 0, \qquad (54)$$

since in a stationary process the expected value of W(+) and W(-) are identical. We also find:

$$\mu_{02} = \left\langle [2\pi(W_R(+) - W_R(-)) - 2\pi\overline{\hat{W}_R(+)} - 2\pi\overline{\hat{W}_R(-)}]^2 \right\rangle$$

$$= 2\pi^2 [\underbrace{\langle \hat{W}_R{}^2(+) \rangle}_{\sigma_W{}^2} - \underbrace{\langle 2\, \hat{W}_R(+)\hat{W}_R(-) \rangle}_{2R(\hat{\xi}', \hat{\eta}')} + \underbrace{\langle \hat{W}_R{}^2(-) \rangle}_{\sigma_W{}^2}]$$

$$= 2\pi^2[2(\hat{\sigma}_W^2 + R(\hat{\xi}',\hat{\eta}'))] \tag{55}$$

$$= 2(2\pi)^2 \sigma_W^2[1 - C(\hat{\xi}',\hat{\eta}')], \tag{56}$$

where

$$C(\hat{\xi}',\hat{\eta}') = \frac{R(\hat{\xi}',\hat{\eta}')}{\hat{\sigma}_W^2}.$$

Here $C(\hat{\xi}',\hat{\eta}')$ is the normalized autocorrelation function. Equation (52) can then be written:

$$\left\langle e^{i2\pi(\hat{W}_R(+) - \hat{W}_R(-)} \right\rangle = e^{-(2\pi)^2 \hat{\sigma}_W^2[1 - C(\hat{\xi}',\hat{\eta}')]} \tag{57}$$

$$= e^{-(2\pi)^2\hat{\sigma}_W^2} + \left(1 - e^{-(2\pi)^2\hat{\sigma}_W^2}\right)C', \tag{58}$$

where

$$C' = \frac{e^{(2\pi)^2\hat{\sigma}_W^2 C} - 1}{e^{(2\pi)^2\hat{\sigma}_W^2} - 1}. \tag{59}$$

When the irregularities have a Gaussian distribution as we have assumed, we can then say several things with respect to Eq. (58).

(a) We have placed no restrictions (yet) on the magnitude of $\hat{\sigma}_W$.

(b) The effective transfer function can be thought of in two parts; a scattered part with an arbitrary autocorrelation function C', and a constant specular component. These components are illustrated in Fig. 5a.

(c) The associated spread function is a delta function with an associated scattering function. The Fourier transform of C' is shown in Fig. 5b.

From Eq. (58) we see that the total flux in the spread function distribution can be divided into two parts, that is,

$$\Phi = \Phi_C + \Phi_H. \tag{60}$$

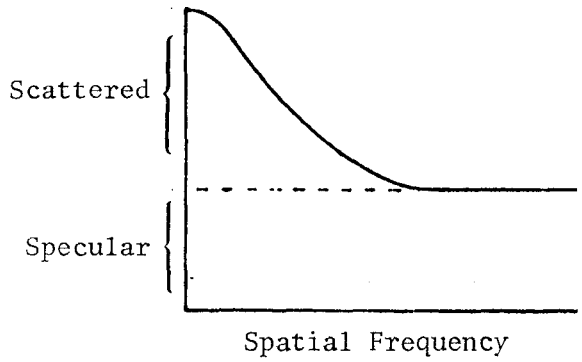

Fig. 5a. Transfer function.

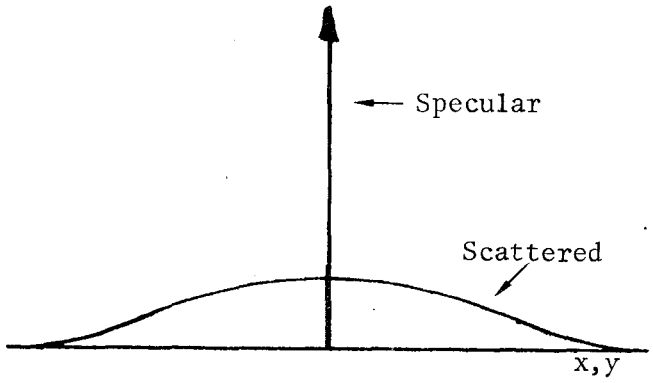

Fig. 5b. Spread function.

The fraction of the light in the specular part is given by

$$\Phi_C/\Phi = e^{-(2\pi)^2\hat{\sigma}_W^2}, \tag{61}$$

and the scattered fraction by

$$\Phi_H/\Phi = 1 - e^{-(2\pi)^2\hat{\sigma}_W^2}. \tag{62}$$

The fractions Φ_H and Φ_C can be determined radiometrically, and the magnitude of the irregularities can be inferred by the consequent relation

$$\hat{\sigma}_W^2 = \frac{1}{(2\pi)^2} \ell n(1 + \Phi_H/\Phi_C), \tag{63}$$

which, as Φ_H/Φ_C becomes small, approaches

$$\hat{\sigma}_W^2 \approx \frac{1}{(2\pi)^2} (\Phi_H/\Phi_C). \tag{64}$$

The shape of the autocorrelation function of the irregularities can be inferred from the measurable scattering function. The function C' in Eq. (59) and the scattering function are a Fourier transform pair, and the desired autocorrelation function C can be obtained from C' by

$$C = \frac{\ell n(1 + (\Phi_H/\Phi_C)C')}{\ell n(1 + (\Phi_H/\Phi_C))} , \tag{65}$$

which, for small Φ_H/Φ_C, becomes simply

$$C \approx C'. \tag{66}$$

This development has shown that it is possible to obtain the statistical properties of mirror surface irregularities by radiometric measurement of the light scattered by the mirror.

III

EXPERIMENTAL APPARATUS AND TECHNIQUE

Apparatus

A schematic diagram of the apparatus used is shown in Fig. 6. To minimize the effects of dust and dirt the equipment was set up in a closed-off area of the Optical Testing Laboratory. The sample and the associated detector optics were further isolated by means of a black velvet tent hung from the ceiling and enclosing the immediate area.

The light source employed was a Spectra-Physics Model 165 Argon Ion Laser. The laser was used in its single-mode configuration with the power adjusted to 20 mw. Two modes of regulation are available in this laser; current regulation and light regulation. In all instances the light regulation mode was used. This mode varies the current supplied by the power supply to assure intensity regulation to within one percent. A further feature of this particular laser is an aperture within the cavity which permits adjustment of the beam diameter. This aperture was set near its maximum opening, 300 μm, to minimize the effects of diffraction.

Light leaving the laser was directed toward the sample by employing two front-surfaced mirrors. The beam then passed through a chopper which modulated the beam at 666 Hz. The chopped light then passed through a single blackened aperture before striking the sample surface. Stray light associated with the laser and light scattered by the beam-directing mirrors and chopper is restricted by this aperture. The sample area is defined by the black velvet tent.

The specular component of the radiation reflected by the sample passes back through the tent. In the case of "normal" incidence the specular beam returned through the aperture by which it entered. The beam in such instances is not precisely normal to the sample surface since it would then effectively become part of the laser cavity and alter the characteristics of the incident beam. Instead the specular and reflected beam are separated by 10 minutes of arc. In the case of non-normal incidence the specular beam passes through a well-defined aperture in the tent and is subsequently directed into a Rayleigh's horn light trap.

The detector in all instances was a Phillip's one-inch end on photomultiplier having an S-20 photocathode. Light reaches the photomultiplier by way of a rigid fiber-optic probe. Such a probe offers several distinct advantages in light sampling. First, substantially the entire cross-section of the fiber bundle is a collector. In addition, the field of view can be restricted to several degrees owing to the propagation properties of fiber bundles, (see Appendix A), and lastly the diameter of the bundle was small compared to that of the photomultiplier allowing both increased angular resolution throughout the scattered field and the ability to probe within half a degree of the incident or specular beams.

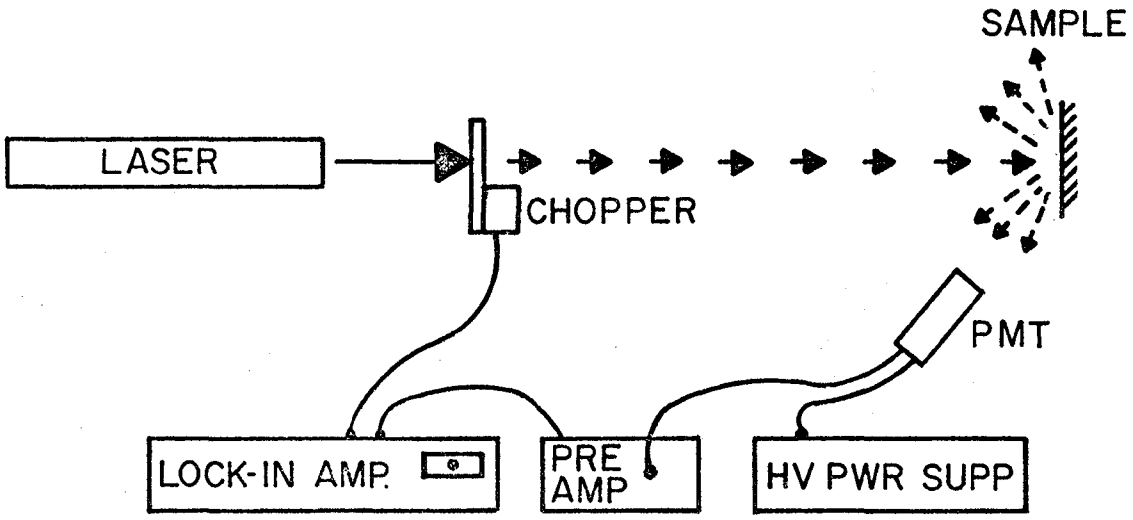

Fig. 6. Schematic diagram of scatter measurement apparatus.

The detector probe unit was mounted on a rigid arm that could be rotated in either of two orthogonal directions. Rotation about a vertical axis was accomplished by means of a massive precision rotary table. In turn the rigid arm was attached to the rotary table by means of a worm gear arrangement which allowed rotation about the horizontal axis. The intersection of these two axes defined the sample location. Figure 7 illustrates this configuration in detail.

The sample holder also had two degrees of rotation; one about the vertical axis and a second about the horizontal axis. The horizontal axis always was in the plane of the sample and the vertical axis always intersected the center of the sample. Alignment of all four axes involved in sample and detector orientation was conducted prior to each experimental run.

Experimental Procedures

The geometry of the measurements is illustrated in Fig. 8. The distance from the sample to the fiber-optic probe is 25 cm. The probe is .3 cm in diameter giving it an angular subtense of .25 degrees.

In order to facilitate a straightforward data reduction routine, only the rotary table was moved during any data run.

The measurement procedure is then as follows: the laser beam is accurately adjusted to strike the center portion of the sample under test by moving the two small mirrors previously mentioned. Subsequently the fiber-optics probe, sample, and rotary table are properly aligned and adjusted with respect to the incident beam. A freshly coated magnesium oxide (MgO) reference sample known to have a diffuse reflectance in excess of ninety-eight percent across the visible spectrum was placed in the sample holder. Scattering measurements from the MgO sample were integrated to calculate the incident intensity of the incoming radiation.

The sample to be measured is then placed in the holder and the scatter field is measured by moving the fiber probe from a position near the specular beam toward the plane of the sample. This motion is accomplished by moving the rotary table in steps toward increasingly larger angles. Typically the scatter was measured at thirty different angles during a given run. At each angle a voltage measurement proportional to the intensity level of the scattered field was recorded. These measurements were then recorded as the ratio of scattered light to reflected light vs. angle from the specular beam. This comprises the raw data.

To compensate for unwanted stray light the sample was entirely removed from its holder and the beam was allowed to exit through the black velvet tent. In this sense the sample can be thought of as perfectly reflecting and any resulting measurements of scattered radiation can then be attributed to background. A background measurement was taken in conjunction with each run. These readings were subtracted from the raw data.

Another source of unwanted light was due to the divergence and finite extent of the laser beam itself.

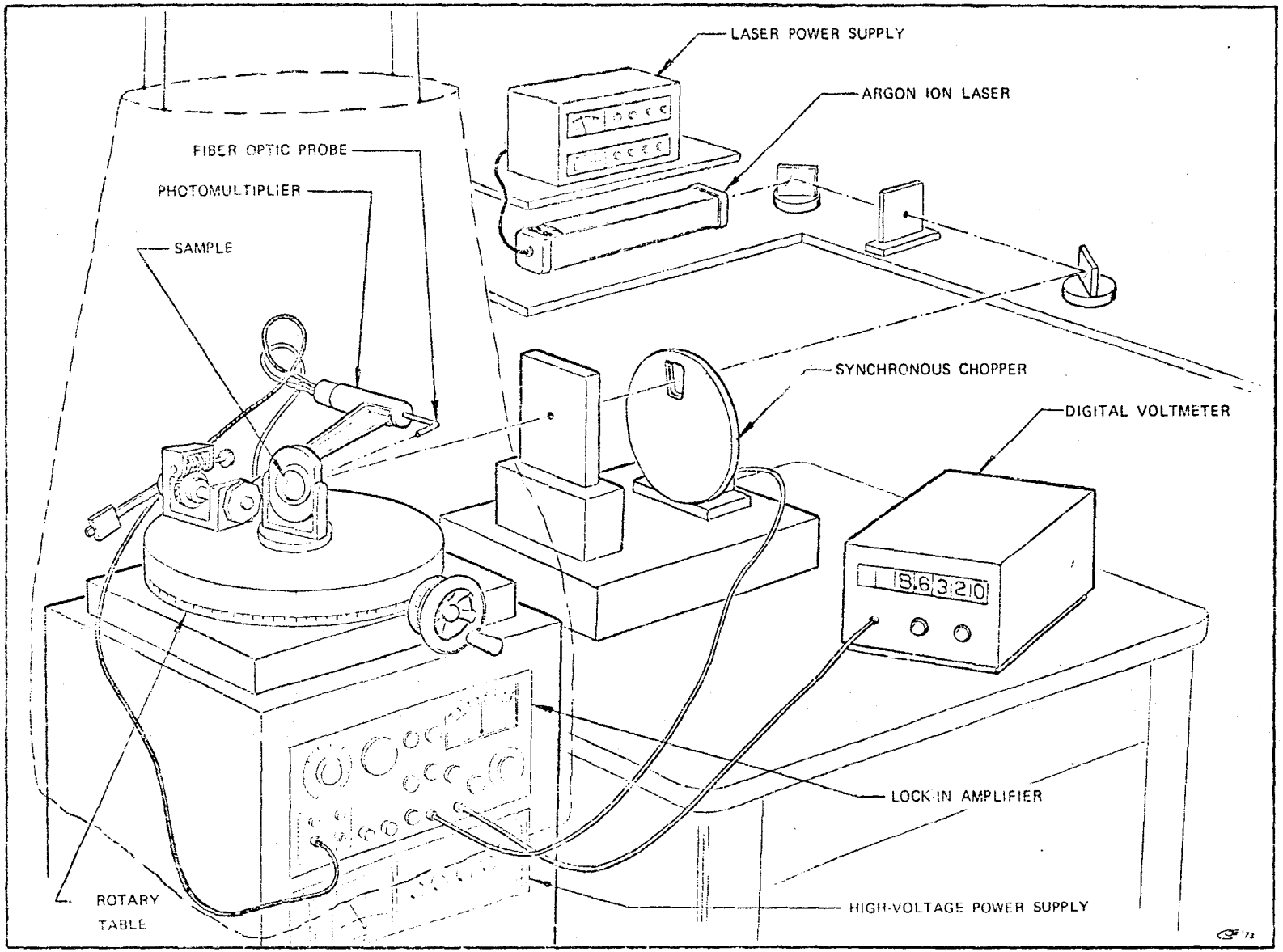

Fig. 7. Drawing of the scatter measurement apparatus.

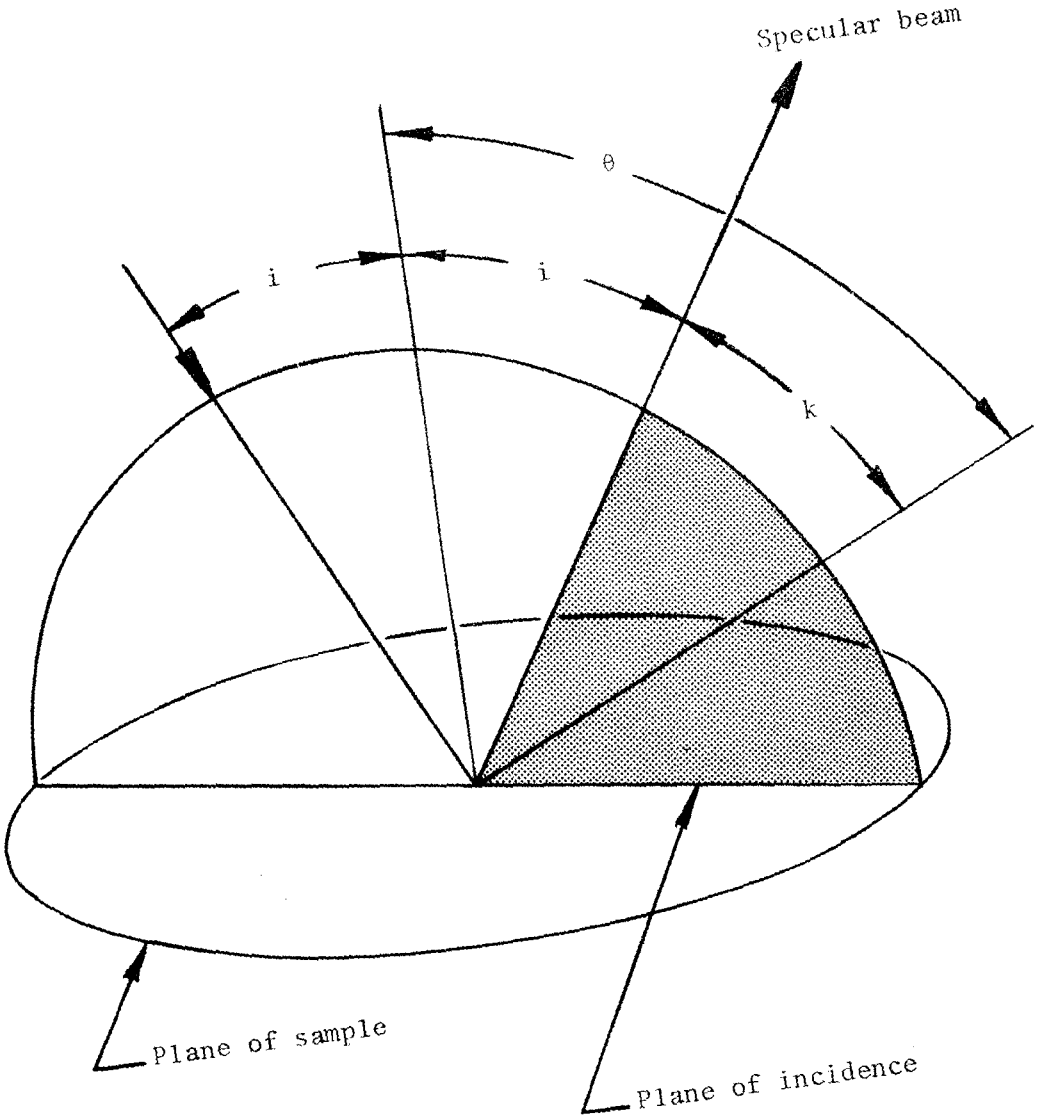

Fig. 8. Geometry of the measurements.

Compensation for the error introduced by beam spread was made in a similar fashion to that used for the background measurements. Again the sample was removed from the sample holder and "no sample" was considered to be the perfect reflector. In this instance, however, the probe was moved to the position of its virtual image as seen when looking into the actual sample. This geometry is shown in Fig. 9. The probe is then moved away from the transmitted beam and measurements are taken at angles corresponding to those taken when the actual sample was in place. These measurements are also subtracted from the initial raw data. They were recorded as "beam-spread" measurements. These measurements became noise limited when the probe was 6 degrees from the incident beam.

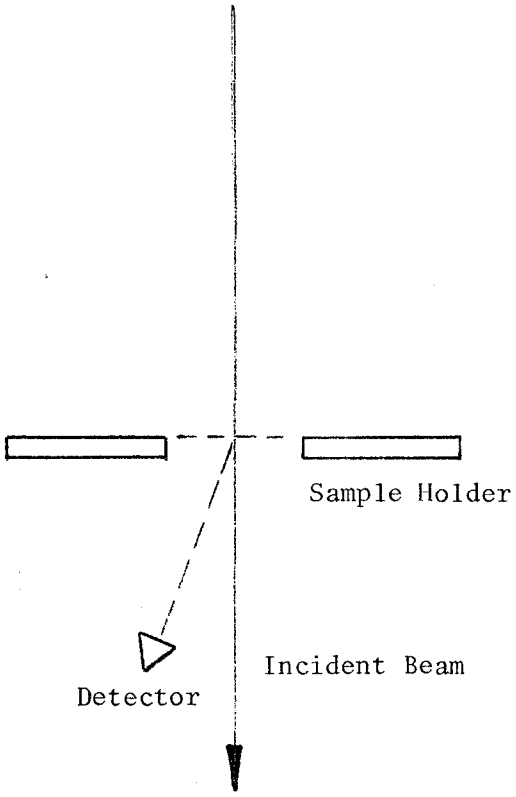

Fig. 9. Geometry of the beam spread measurements.

IV

DATA AND RESULTS

The distribution of light scattered by a plane mirror as a function of surface roughness, angle of incidence, and wavelength are reported in this section. General results are compared with the theory.

Background Data

As noted in the section on Experimental Procedure, the background measurements were due to spread of the laser beam. As these measurements were all taken through the sample holder with no sample in place, it was expected that all measurements would be the same. Figures 10 and 11 show, however, that the values of the background varied considerably. The cause for these background differences is not clear, but several things should be pointed out with respect to them. First, the angular extent of the background is confined to within eight degrees of the specular beam, with most detail of any note being within six degrees of the specular beam. In some cases the small angle data has a shape very similar to that of a particular background measurement, and in others there is no strong correlation. The net result is that these background measurements, which should all be identical, reduce our confidence in the small angle data (that data between 1.5° and 6°). Data taken outside this range appears to be reliable.

Because of discrepancies in the background measurements we have presented much of the data in a dual format. In the first format we subtracted the background that was taken in conjunction with the particular set of measurements. The second format presents the data with the "best-fit" background subtracted.

Presentation of the Data

A measure of the total flux, Φ, incident on the samples was obtained by performing a numerical integration of the scattered light distribution from the magnesium oxide reference sample. These integrations were made in conjunction with each set of measurements.

Background data describing the flux distribution of the incident beam is then subtracted from measurements of the intensity of the scattered field. These data are represented by η'. The corrected data is then normalized by dividing by Φ and the data from each run can now be plotted to yield the scattered light distribution of the sample.

These distributions are plotted as modified log-log plots with the ordinate being log $\eta/\cos\theta$ (where $\eta = \eta'/\Phi$ is the scatter coefficient); where θ is the angular position of the measurement with respect to the normal to the sample. The abscissa in these plots is log ($\sin\theta$ - sin i); where i is the angle of incidence (see Fig. 8). We now have $\theta = k+i$, k being the angle

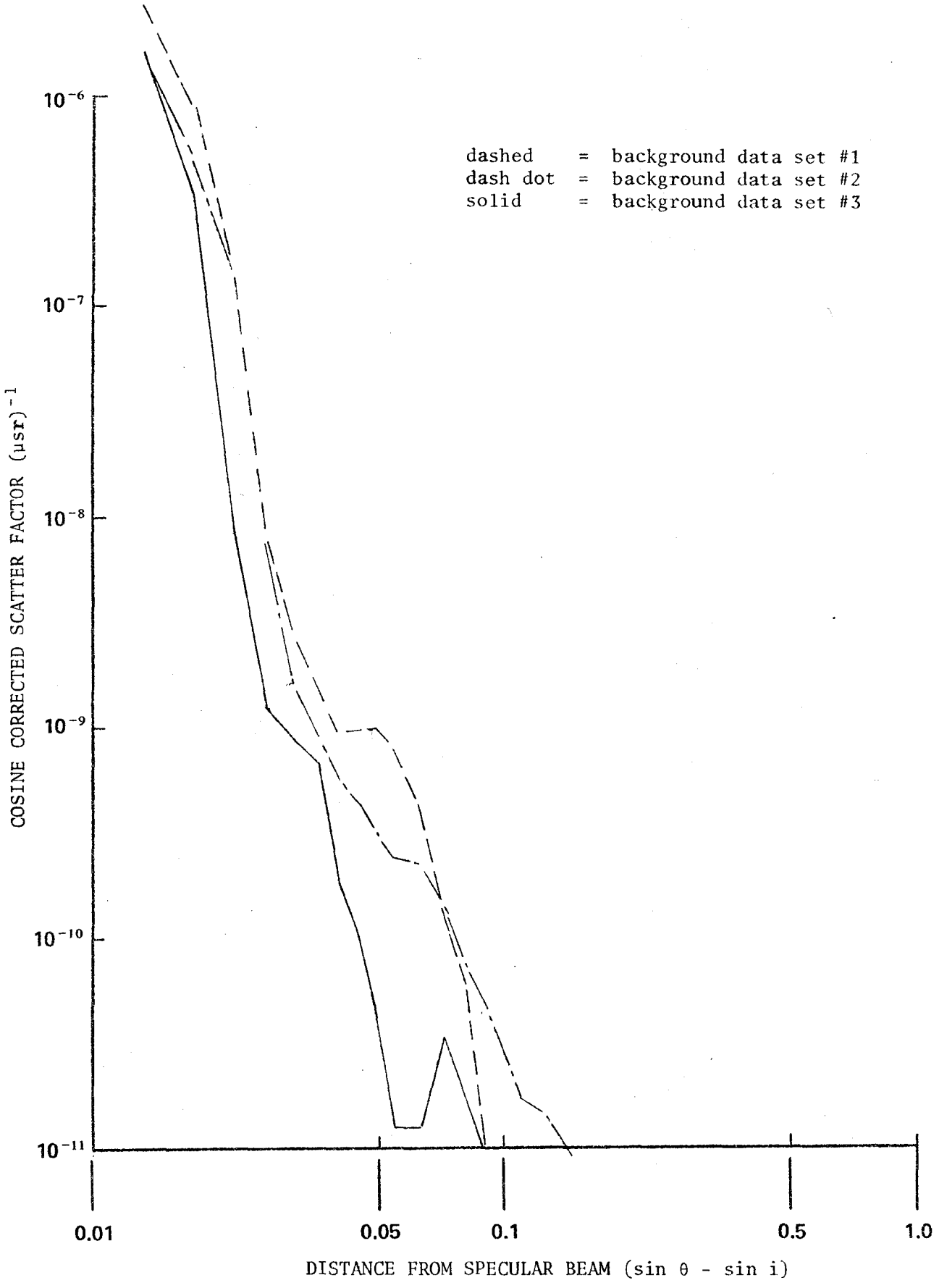

Fig. 10. Measurements of the background due to beam spread.

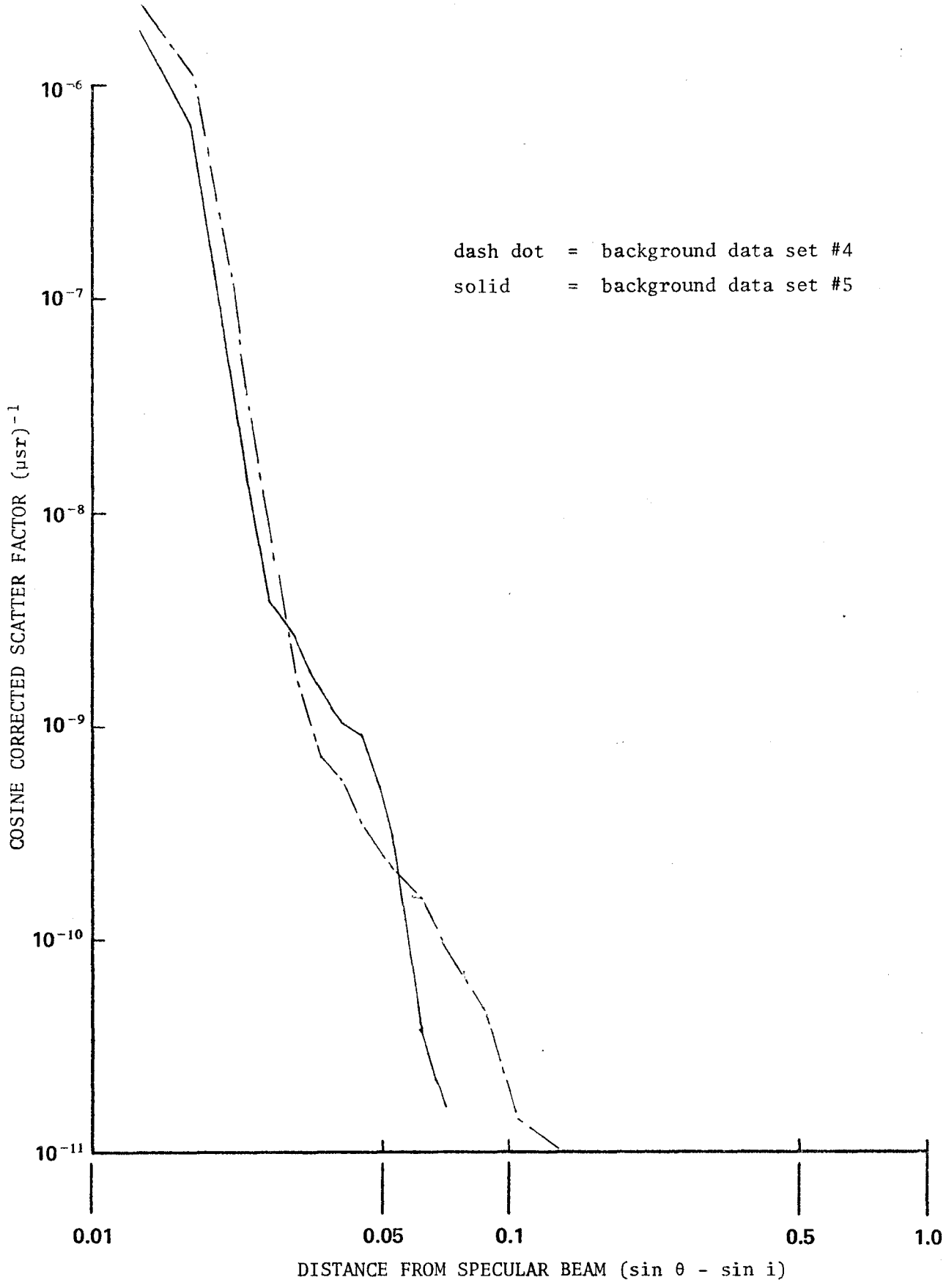

Fig. 11. Measurements of the background due to beam spread.

from the specular beam to the measurement. To illustrate the effect that these plotting coordinates exercise on the data, intermediate steps are illustrated in Figs. 12, 13, and 14 for samples 247 and MgO.

Figure 12 is a log-log plot of η vs. the angle k from the specular beam. In Fig. 13 we have plotted the same information, however, we have now divided the scattered flux by $\cos\theta$. The effects of this division are seen easily at the larger angles where $\cos\theta$ is small and the plotted values are noticeably higher. The result of this division is of particular note in the case of the MgO sample where the curve has become almost flat. (A flat plot would indicate a perfect Lambertian surface.)

Figure 14 illustrates the change of scale in the abscissa when we shift from log (k) to log ($\sin\theta$ - sin i). In this case we have used data for i = 0° and i = 45° from sample 247. The change in scale for normal incidence measurements can be noted for both MgO and sample 247.

The data, at least in the large-angle region where it is well-behaved, appears to follow an inverse power law, and must eventually level off to a finite maximum value for very small angles, although this leveling does not show in the data. A function that may be used to represent this behavior is

$$I = I_o[1 + (\rho/\rho_o)^2]^{-(s/2)}, \tag{67}$$

where I_o is the central maximum radiant intensity, $\rho = \sqrt{\alpha^2+\beta^2}$ is the direction cosine of the scattering angle (assuming the scattering function is a figure of revolution), ρ_o is a scale factor measuring the width of the scattering function, and s is the rate at which the function decreases for large angles. For small angles where $\rho/\rho_o \ll 1$,

$$I \approx I_o[1 - \tfrac{s}{2}(\rho/\rho_o)^2], \tag{68}$$

and for large angles where $\rho/\rho_o \gg 1$,

$$I \approx (I_o\rho_o{}^s)\rho^{-s}. \tag{69}$$

The total flux scattered out to a radius ρ^* is given by

$$\Phi_s(\rho^*) = 2\pi\int_0^{\rho^*} I\rho d\rho = \frac{2\pi I_o\rho_o{}^2}{2-s}\left\{[1 + (\rho^*/\rho_o)^2]^{\frac{1}{2}(-s)} - 1\right\}, \quad s < 2, \tag{70}$$

and the total flux scattered, $\Phi_s(1) = \Phi_H$, is obtained by setting $\rho^* = 1$.

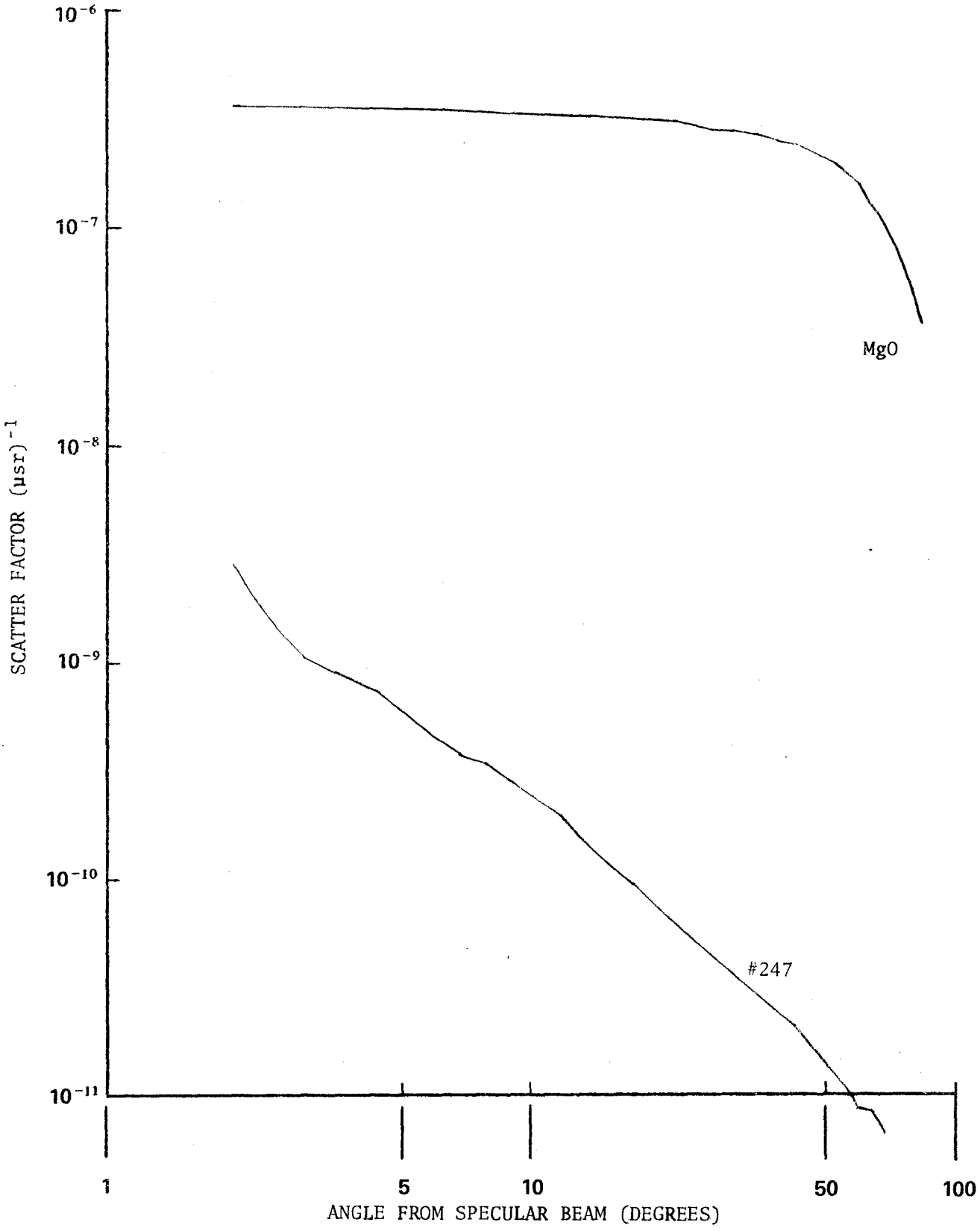

Fig. 12. Scatter vs. angle from specular beam; normal incidence.

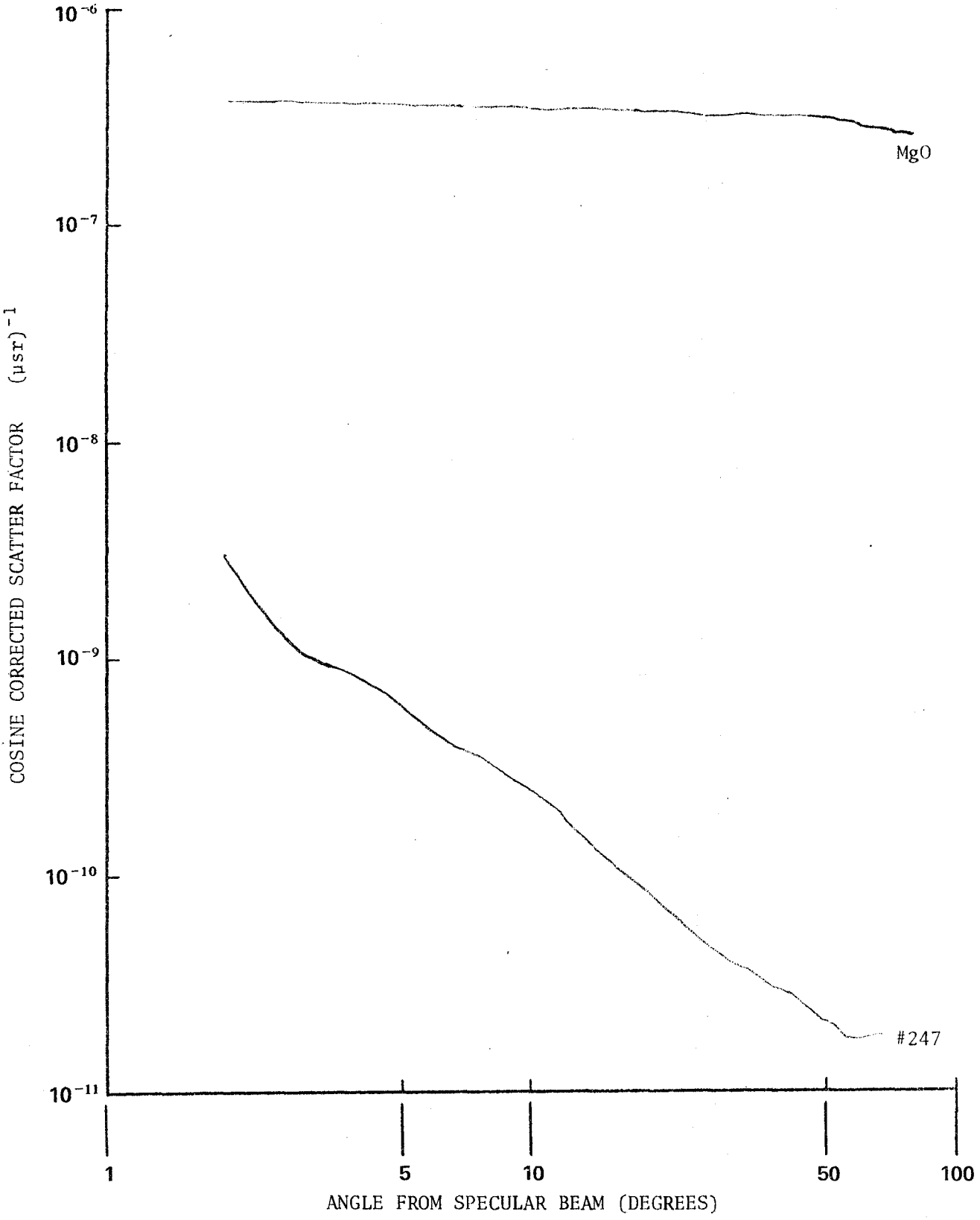

Fig. 13. Scatter vs. angle from specular beam; normal incidence.

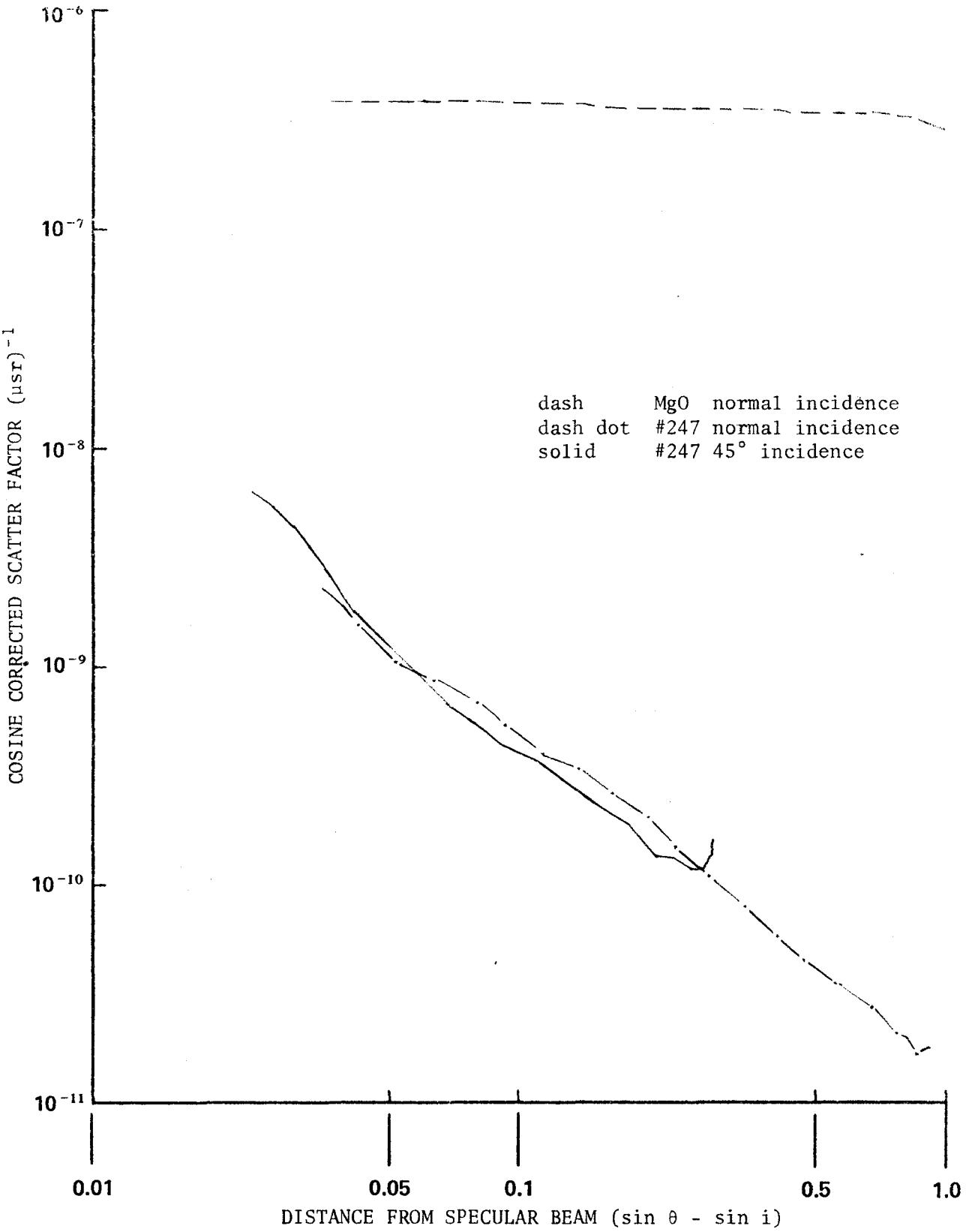

Fig. 14. An example of scatter data plotted vs. the distance from the specular beam.

In the limit for $\rho_o << 1$, we obtain

$$\Phi_H \approx \frac{2\pi I_o \rho_o^s}{2-s} . \tag{71}$$

If we compare this with Eq. (69), we see that we can obtain an approximate value for the total scattered flux by the relation

$$\Phi_H \approx \frac{2\pi}{2-s} I(1), \tag{72}$$

without knowing the values of I_o and ρ_o.

Scatter as a Function of Surface Roughness

Variations in surface roughness were obtained by employing a variety of grinding polishing techniques as outlined in Appendix A. The scattered light distributions of all samples listed in Table 3, Appendix A, were measured at normal incidence. The results of these measurements are shown in Figs. 15 and 16.

It should be noted that the slope of the wide angle portion of the polished samples is close to being flat for the angles beyond six degrees. The slopes vary from about 1.25 to 2.0. Also of significance is the change of shape brought about by subtracting the appropriate background. Selection of this background appears to have substantially removed the anomaly in the plots of samples 236, 222, 247, and EDF 3-4.

Samples 221 and 229 are ground samples and exhibit a behavior close to that of MgO. No specular beam was detectable when these samples were illuminated at normal incidence.

Separate scattering phenomena may account for the kink in the plots of polished samples at approximately six degrees. However, uncertainty of the background data necessitates further research to determine if this is true.

Scatter as a Function of Angle of Incidence

In the general case, light is not normally incident upon an optical surface. The behavior of scattered radiation when light is incident upon a sample at angles between 0° and 60° was investigated. In all cases the measurements were made in the plane of incidence and only include measurements in the shaded portion of Fig. 8. (A modification to the existing apparatus is suggested, [see "Suggestions for Future Research"] that will allow measurement throughout the plane of incidence and planes orthogonal to the plane of incidence.)

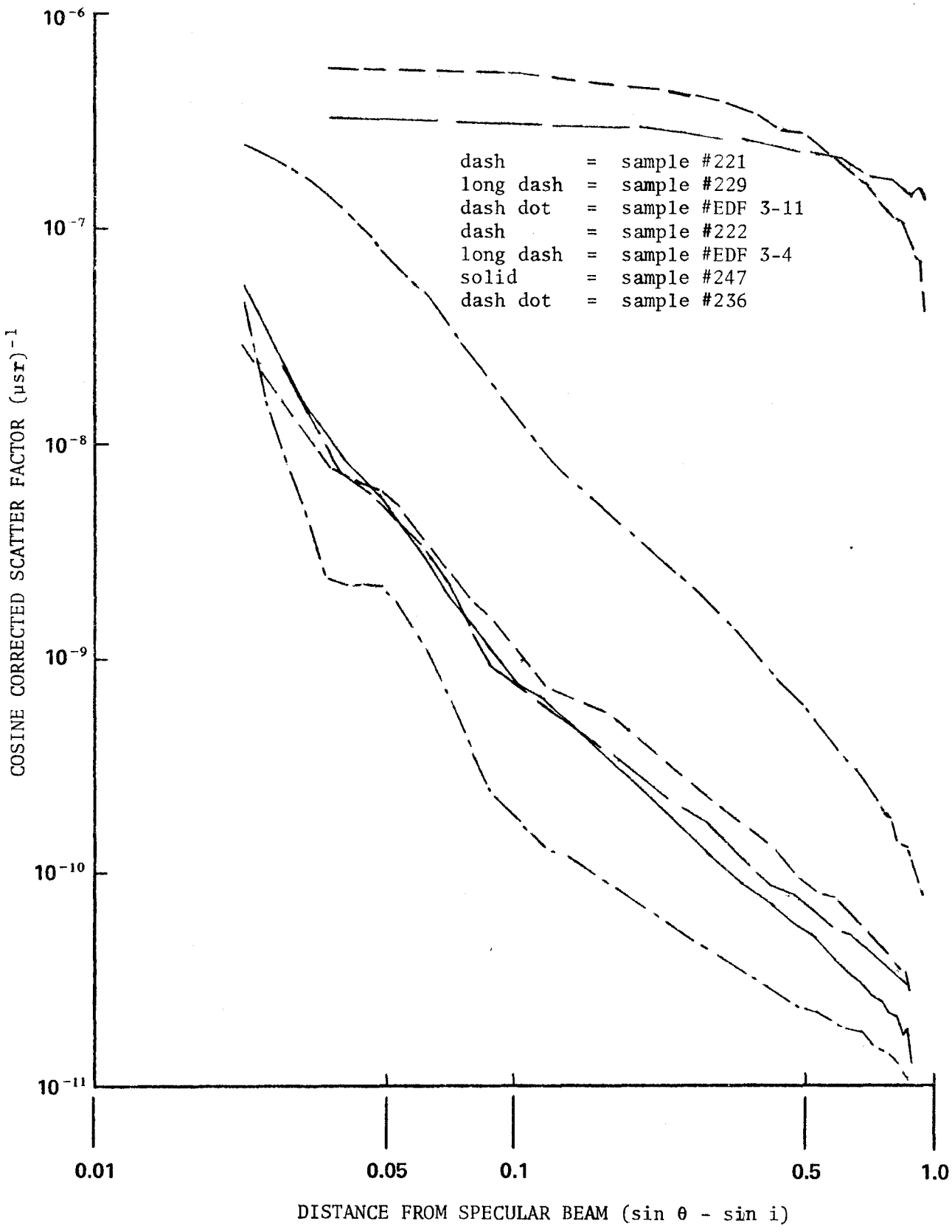

Fig. 15. Scatter as a function of surface roughness, normal incidence; corrected for background measured in conjunction with this data.

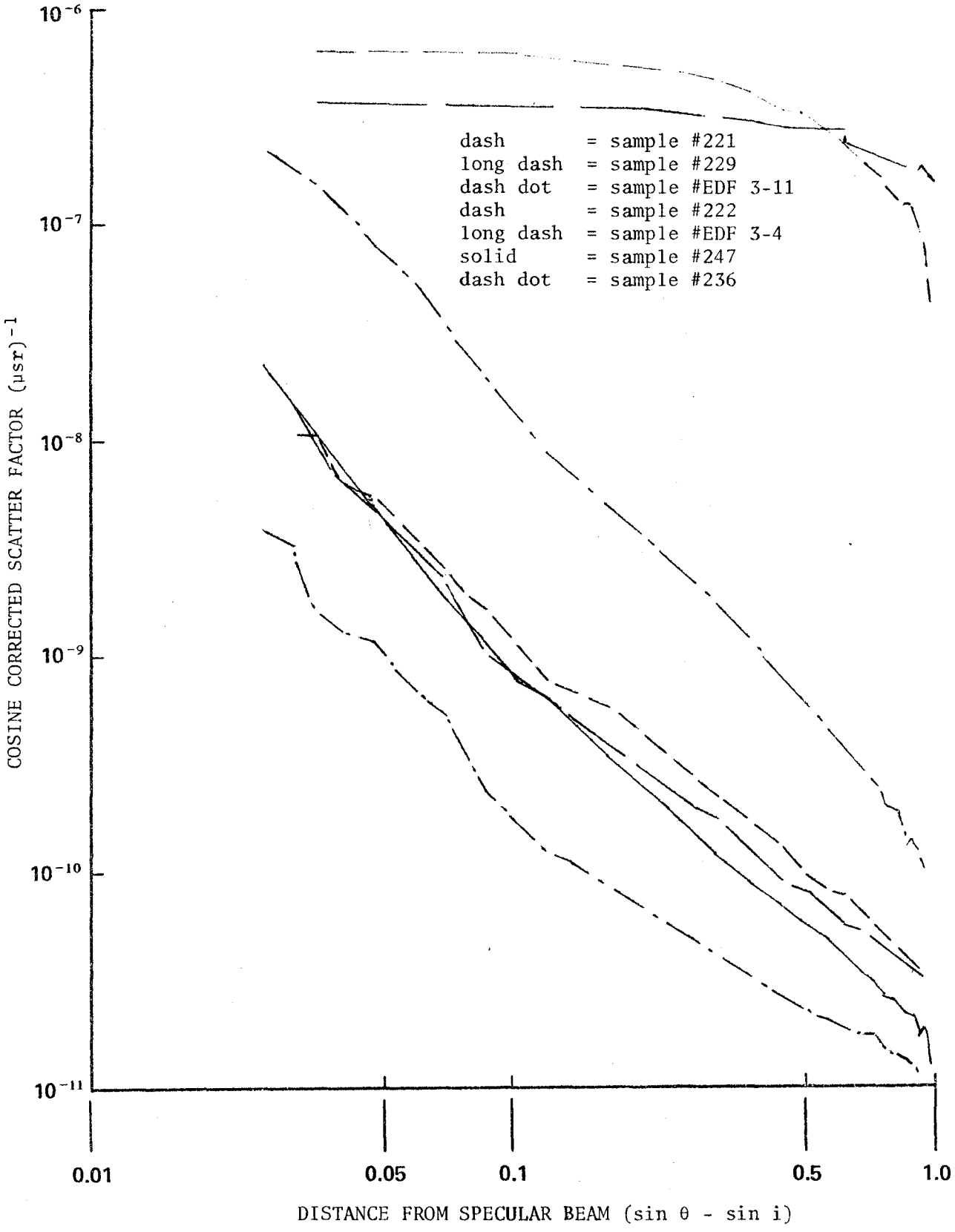

Fig. 16. Scatter as a function of surface roughness, normal incidence; corrected for best fit background (see discussion).

The results of a series of measurements, with the beam incident at various angles, is shown in Figs. 17 and 18. In Fig. 17 a strong anomaly is present, which is substantially removed when a more judicious background is selected as shown in Fig. 18.

The slopes of these curves is close to 1.5. In Fig. 18 the individual curves exhibit close agreement with each other. More extensive research should be pursued to substantiate this type of agreement.

Scatter as a Function of Wavelength

An original intent of the research reported here was to measure the scattered light distribution of samples at two different wavelengths: one in the visible portion of the spectrum and a second in the mid-infrared. As research progressed, it became evident that satisfactory results could not be obtained if the original wavelength regions were retained. A decision was made to use two wavelengths in the visible portion of the spectrum for the following reasons:

(1) Two measurements in such widely separated regions of the spectrum would require that the separate laser sources be used. It is unlikely that these sources could be aligned to illuminate identical portions of the sample under test.

(2) In order to measure the light levels associated with wide angle scatter, two separate detectors are necessary. It is difficult to insure that the absolute energy and the collection area of each detector be well known.

(3) A reference sample that would be useful in both the infrared and visible was unknown.

In contrast, the availability of an argon-ion laser simplified the associated problems of measurement immediately. A prism internal to the cavity of the laser permits selection of several laser lines without the alteration of beam direction. The lines used were 514.5 nm (green) and 459.0 nm (blue). A photomultiplier exhibits good response at each of the available lines allowing a single detector configuration to be used for both wavelengths. Furthermore, the diffuse reflectance of MgO exceeds .98 throughout the spectral region of the laser. This allowed an MgO sample to be used as a reference. Detector response, laser power output, reflectance of intermediary mirrors, and transmittance of the fiber-optic probe could all be reduced to a single proportionality factor. This factor is obtained by taking the ratio of the integrated diffuse reflectance of the MgO reference at the two wavelengths of concern.

To measure relative scatter as a function of wavelength, an MgO reference sample is placed in the sample holder. Its diffuse reflectance is measured at the first of the two wavelengths. The reference is removed from the sample holder and replaced with the sample under study. The diffuse reflectance of the sample is then measured at the first wavelength. The laser is then tuned to the second of the chosen wavelengths, and the diffuse

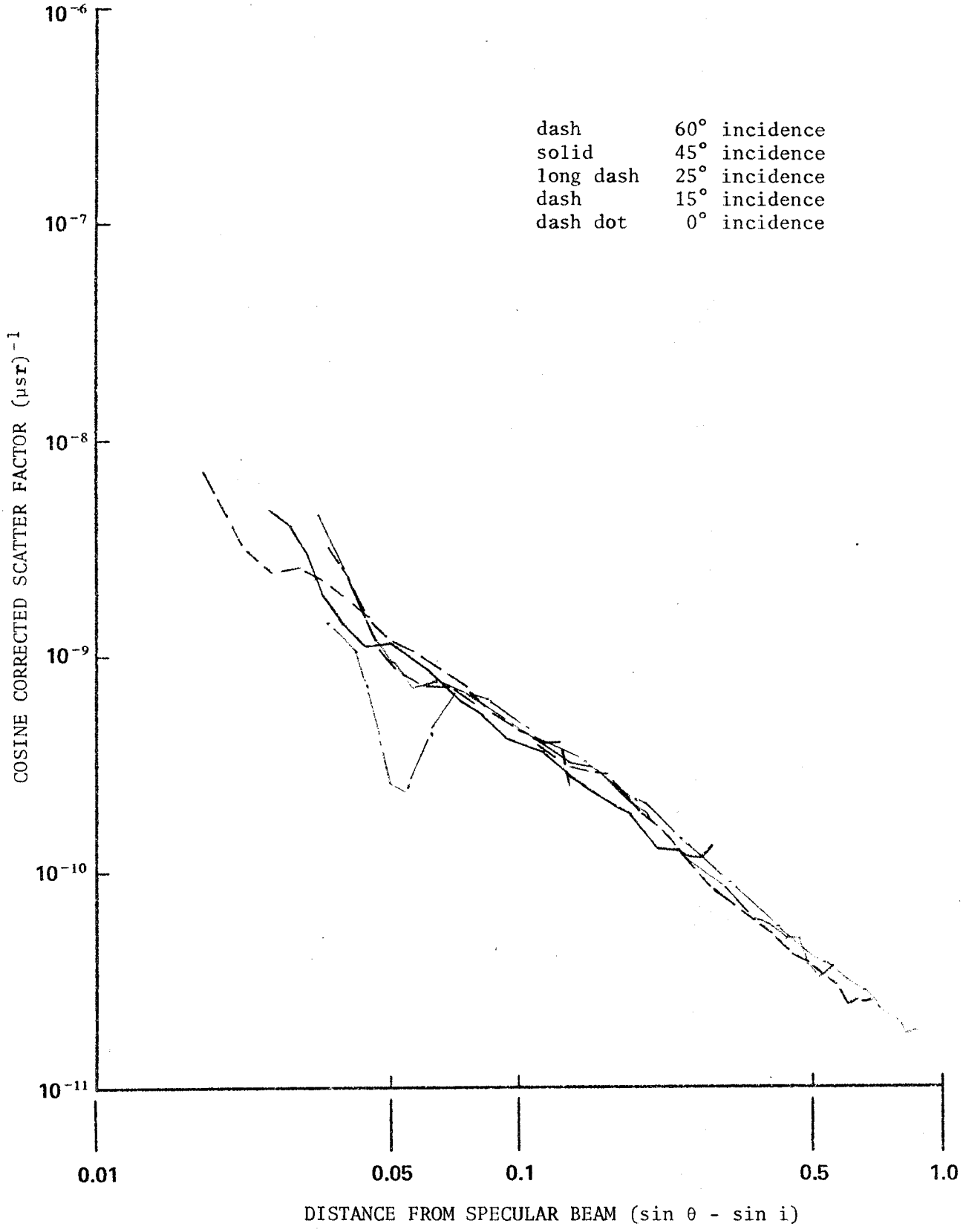

Fig. 17. Scatter from sample #247 as a function of angle of incidence corrected for background measured in conjunction with this data.

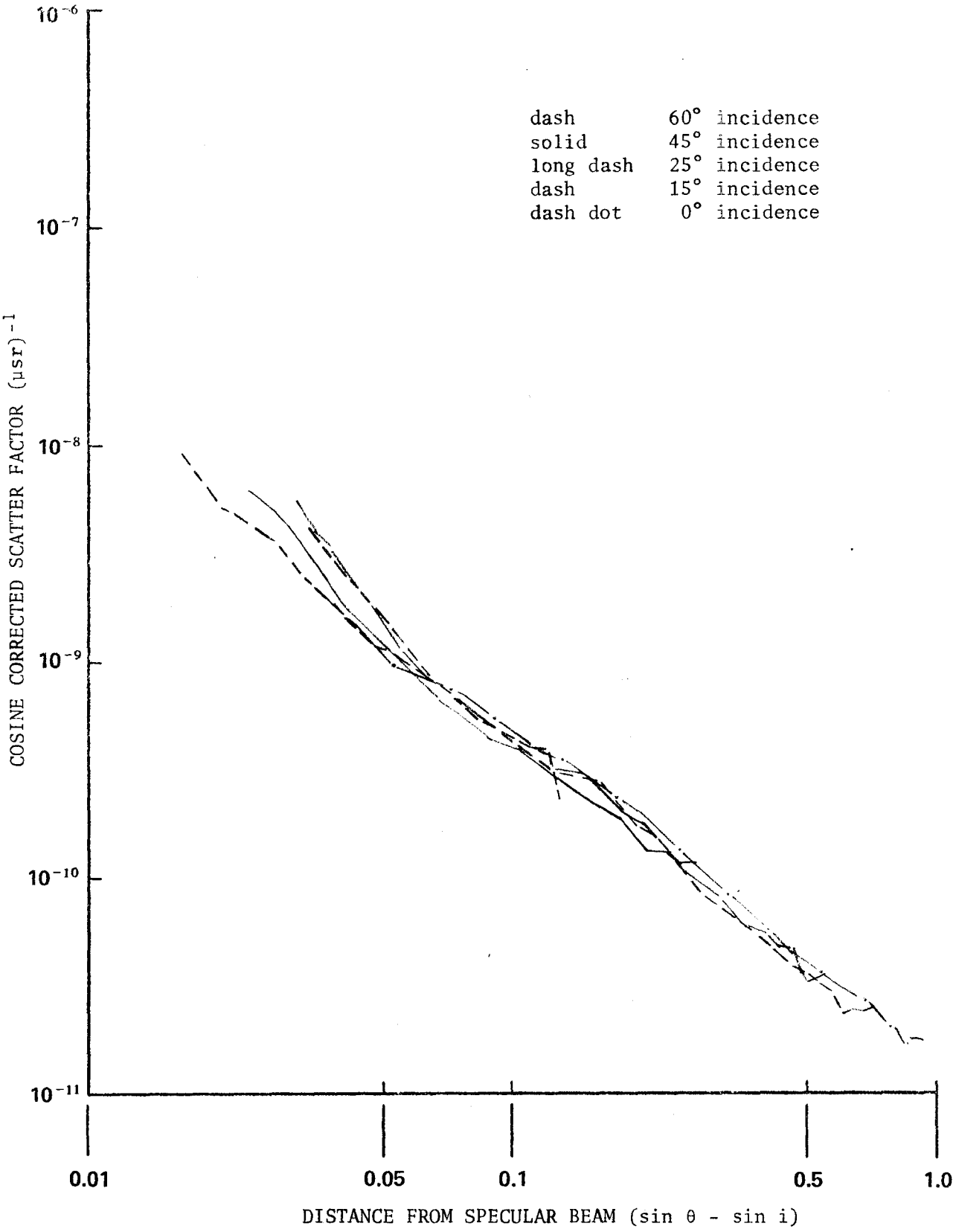

Fig. 18. Scatter from sample #247 as a function of angle of incidence corrected for best fit background (see discussion).

reflectance is measured at this wavelength. (It should be noted that the change of wavelength does not alter the position of any optics outside the laser cavity, and that the laser beam in both cases strikes the same portion of the sample.) The test sample is now replaced by the reference sample in the sample holder, and the diffuse reflectance of the reference at the second wavelength is measured.

A numerical integration performed on the data taken from the reference measurements yields the relative intensity of the incident radiation with the thru-put of the entire system (reflectance, transmission, photocathode response and electronics) taken into account. The ratio of the resultant integrations is a scale factor that is then used to "correct" the measurements from the test sample for all effects except for wavelength. The result of these measurements is shown in Figs. 19, 20, &21. All measurements were made at normal incidence.

In order to predict the wavelength dependence of the scattering function for large angles, we first combine Eqs. (69) and (71), obtaining

$$I = \frac{2-s}{2\pi} \Phi_s(1) \rho^{-s}. \tag{73}$$

The form of the scattering function should not vary with wavelength, so the slope s should not be dependent on wavelength. Furthermore, if the scattered fraction of the flux is small, the total scattered flux is given by

$$\Phi_H = 1 - e^{-(2\pi)^2 \hat{\sigma}_w^2} \approx (2\pi)^2 (\sigma_w/\lambda)^2, \tag{74}$$

so that Φ_H, and therefore I, should vary inversely as the square of the wavelength. This is consistent with the data.

Numerical Integration of the Scattered Light Distributions

A numerical integration of the scattered light distribution yields Φ_H, the net scattered flux if we can assume the distribution is rotationally symmetric, and that the contribution due to the fraction of light not included in the integral is small. These assumptions appear reasonable as we have no evidence to the contrary. The results of these integrations are listed in Table 1.

Further, from the theory we know that the rms surface roughness, $\hat{\sigma}_w$. is given by

$$\hat{\sigma}_w^2 = \frac{1}{(2\pi)^2} \ell n \left(1 + \frac{\Phi_H}{\Phi_C} \right). \tag{75}$$

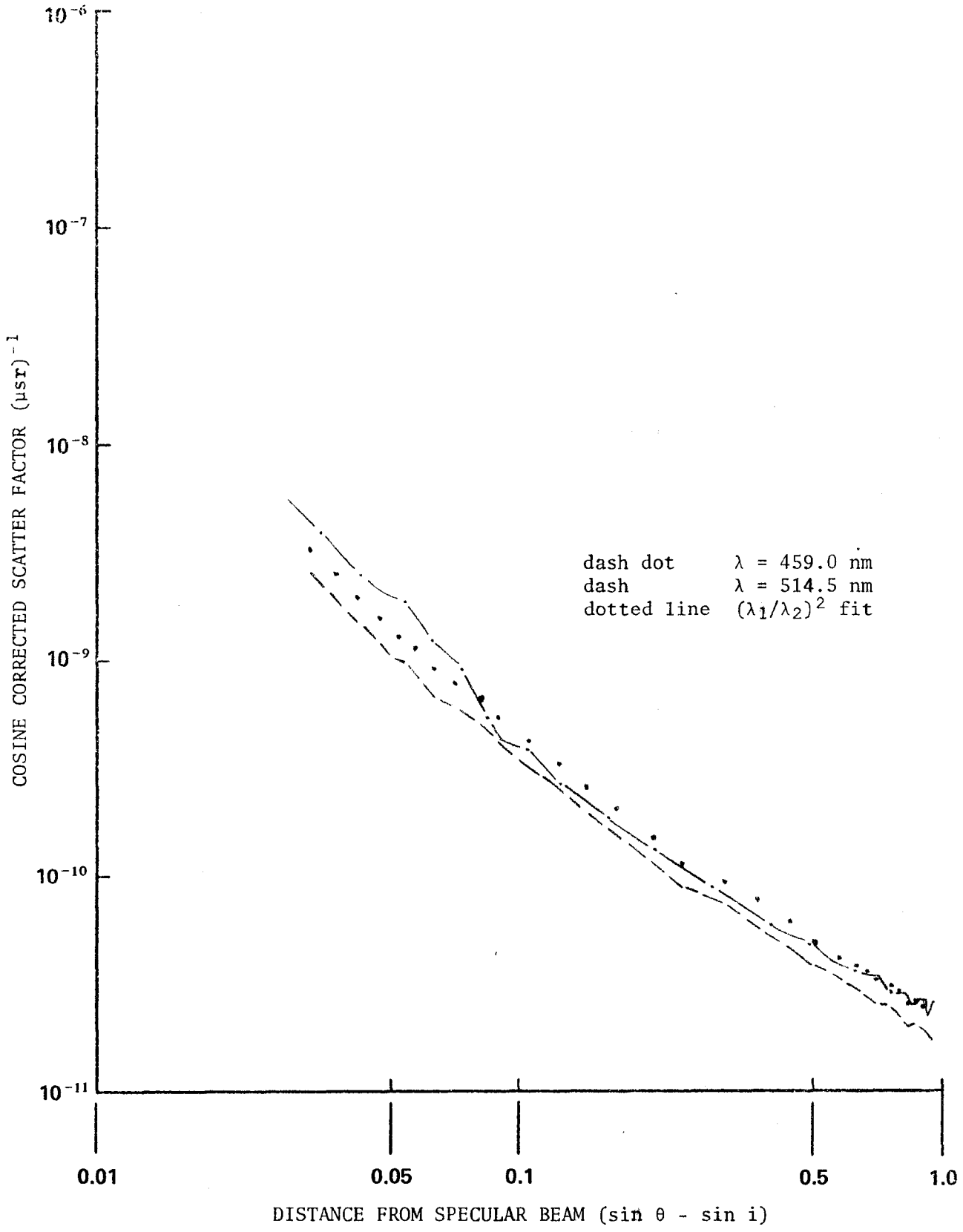

Fig. 19. Scatter as a function of wavelength, sample #236.

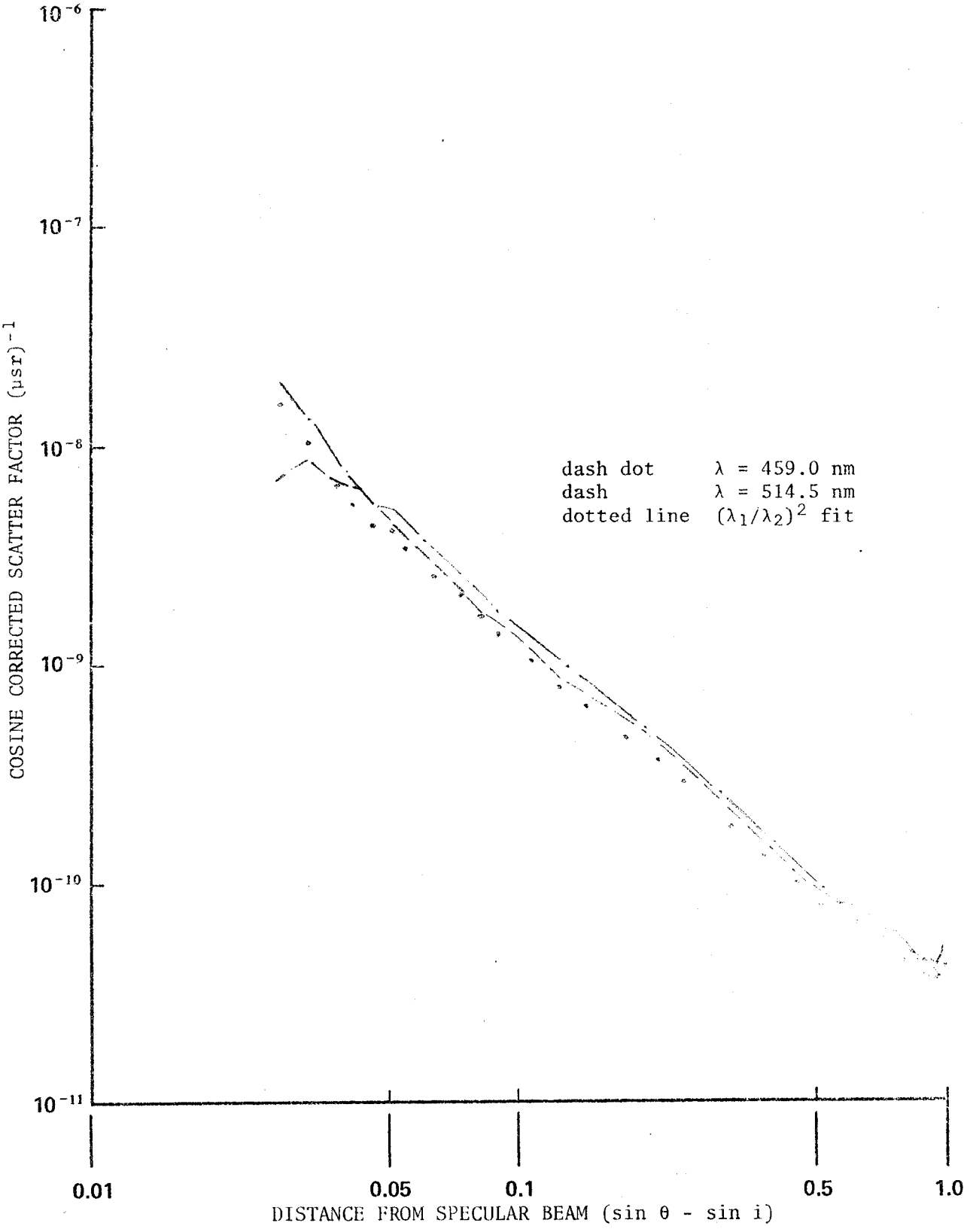

Fig. 20. Scatter as a function of wavelength, sample #247.

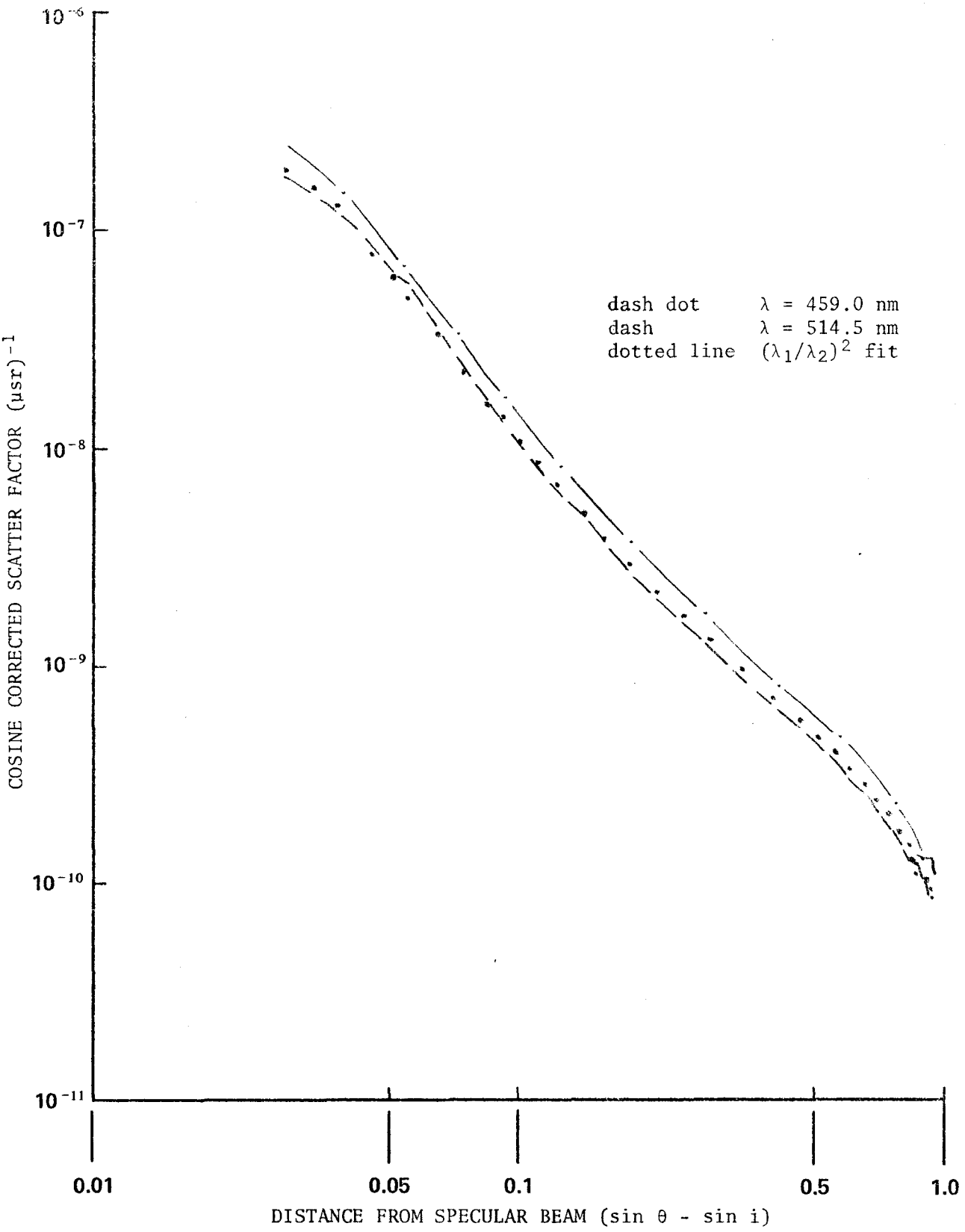

Fig. 21. Scatter as a function of wavelength, sample #EDF 3-11.

Since $\Phi = \Phi_H + \Phi_C$, we can make the assumption that $\Phi_C = \Phi$ when Φ_H is very small. This is the case for all but the two ground surfaces, samples 221 and 229. The rms roughness is then given by

$$\sigma_w^2 \cong \frac{1}{(2\pi)^2} \ell n\left(1 + \frac{\Phi_H}{\Phi}\right) \lambda^2. \tag{76}$$

Calculations of σ_w are given in Table 2. These results exhibit an order of magnitude agreement with the estimated roughness values.

TABLE 1

RESULTS OF THE NUMERICAL INTEGRATION

OF THE SCATTERED LIGHT DISTRIBUTIONS

Sample No.	Integrated Scatter (%)
236	0.014
247	0.033
EDF 3-4	0.038
222	0.046
EDF 3-11	0.38
229	69.5*
221	71.1*

*In the case of the ground samples, no specular beam was apparent and these figures represent the total diffuse reflectance.

TABLE 2

CALCULATED RMS SURFACE ROUGHNESS, σ_w

Sample No.	Φ_H/Φ	σ_w (nm)
236	0.00014	0.95
247	0.00033	1.5
EDF 3-4	0.00038	1.6
222	0.00046	1.8
EDF 3-4	0.0038	5.1

V

SUGGESTIONS FOR FUTURE RESEARCH

In conducting the research presented in this report several ideas for improving the measurements and our understanding of surface scattering have been kindled. These ideas are summarized below.

(1) A redesign of the existing apparatus is possible that will allow one to scan through the specular beam and thus make measurements over the entire plane of incidence. This can be accomplished by introducing an offset into the fiber-optic probe.

(2) Through the use of a lens to focus the incident laser beam onto the hemisphere an exact Fourier transform can be formed. Approximations involving the quadratic phase factor can then be eliminated.

(3) An investigation of surface profiles using the techniques of stereo-electron microscopy could yield more accurate measurement of auto-correlation function and the surface height distribution.

(4) Surfaces that are partially polished, and surfaces that are polished and then partially ground as well as materials other than glass should be investigated.

APPENDIX A

SAMPLE PREPARATION

This section deals with sample selection, polishing, cleaning and coating. An original goal of the research reported here was to choose samples that bracketed the types of surfaces typically produced in optical component manufacture. Coatings for these surfaces we produced were carefully controlled and in all cases we believe had less effect on overall scatter than did the condition of the substrates. All surface roughnesses are reported as a combination of coating plus substrate roughness.

Substrate Materials and Preparations

Samples used in these experiments were of two different types of glass. The hardness range of conventional optical glass was well bracketed by the choice of substrates. The large majority of the substrates were made of fused silica of the Homosil trademark. These substrates were of exceptional quality and essentially free from bubbles and sleeks. All substrates were 3.17 cm in diameter and 0.63-cm thick. Fused silica is one of the hardest of the conventional optical substrates. The remaining substrates were made of optical quality extra dense flint glass. The particular category in this case is known as EDF3. EDF3 is one of the softest optical glasses and it was chosen as a substrate for this particular reason.

Surface preparation of the different samples is outlined in Table 3. All samples were finished to be closely flat. Grinding and polishing procedures are more closely described by Mott (1971) and Orme (1972). Surface roughness in the samples varied from 1.0 nm to 3,000 nm. The EDF3 samples were much more prone to small scratches as might be expected. In all, thirty-two samples were prepared and of these, eight were selected for investigation.

Cleaning

The prepared samples were cleaned prior to coating with aluminum. Cleaning consisted of careful washing with Liquinox, a mild detergent, under very warm, filtered tap water. Such soaping was repeated three times for each individual sample. Samples were then mounted in a sample holder while held in distilled water. Once in a holder, samples were moved to an ultrasonic cleaner filled with distilled water for rinsing. Purity of the distilled water in the ultrasonic cleaner was monitored through resistance measurements. The water was changed several times, until it was substantially as pure as it was before the samples were added. Once rinsed the samples were set to dry in a dust-free atmosphere. Dry samples were removed from the sample holders and placed in individual boxes being supported by the edge of their backside. Mott (1971) used a similar cleaning technique, which he describes more completely.

Coating

Cleaned dry samples were then placed in a high vacuum chamber and coated to opacity with pure aluminum. Coating technique varied from the standard only in that excessive care was taken to allow the chamber to reach a pressure below 2×10^{-6} torr prior to coating. Opacity was monitored by watching the extinction of the tungsten evaporating filament through the substrates. The samples were allowed to cool to room temperature prior to removal from the chamber. Each coating run contained ten different samples. Once coated, samples were returned to their individual storage boxes. After all samples were coated, the best samples of each type were selected for measurement. This selection was made on the basis of individual inspection of each sample while held under a microscope illuminator in an otherwise dark room. Samples that had coating nonuniformities, sleeks or pinholes were rejected as were those with waterspots, large scratches of otherwise questionable appearance. Prior to each scatter measurement run, samples were again individually inspected for flaws. Dust was removed using a commercially available pressurized air can. After each sample was measured for scatter, it was returned to its individual box.

TABLE 3

SURFACING PROCEDURES AND ROUGHNESSES

Sample Number	Substrate Material	Lap Material	Polishing Medium	Polishing Time	Force Applied kg/cm^2	Approximate Surface (nm) Roughness
236	Quartz	Optical Quality Pitch	CeO*(milled 2000 hr)	8 hr	.2	1.0
			Distilled H_2O* w/same lap	8 hr	.2	
247	Quartz	Wood (end cut fir)	CeO (unmilled)	4 hr	.3	4.0
222	Quartz	Plate Glass	Al_2O_3(1μm diam)	1 hr	.12	12
221	Quartz	Cast Iron	Al_2O_3(2μm diam)	20 min	.15	100
229	Quartz	Cast Iron	Al_2O_3(30μm diam)	20 min	.15	1500
EDF3-4	EDF-3	Optical Quality Pitch	CeO(milled 2000 hr)	8 hr	.12	2.5**
			H_2O*(distilled w/same lap)	8 hr	.12	
EDF3-11	EDF-3	Optical Quality Pitch	CeO (milled 500 hr)	4 hr	.12	15**

*Closed circulation system.

**Soft glasses exhibit a strong tendency to scratch and sleek.

APPENDIX B

PROPERTIES OF THE FIBER-OPTIC PROBE

The fiber-optic bundle offers several unique advantages in the collection of the scattered radiation. Being rigid, it is self-supporting and, in effect, transfers the detector to the end of the fiber bundle. Furthermore, being small in cross-section, one is allowed to probe the space near the specular direction without the detector scattering light back towards the sample. Finally, fiber-optic bundles have the property that off-axis light leaves the bundle both attenuated and distributed away from the normal direction. Figures 22 and 23 illustrate this. Correct baffling between the end of the fiber-optic bundle and the detector can then eliminate much of the stray and background radiation.

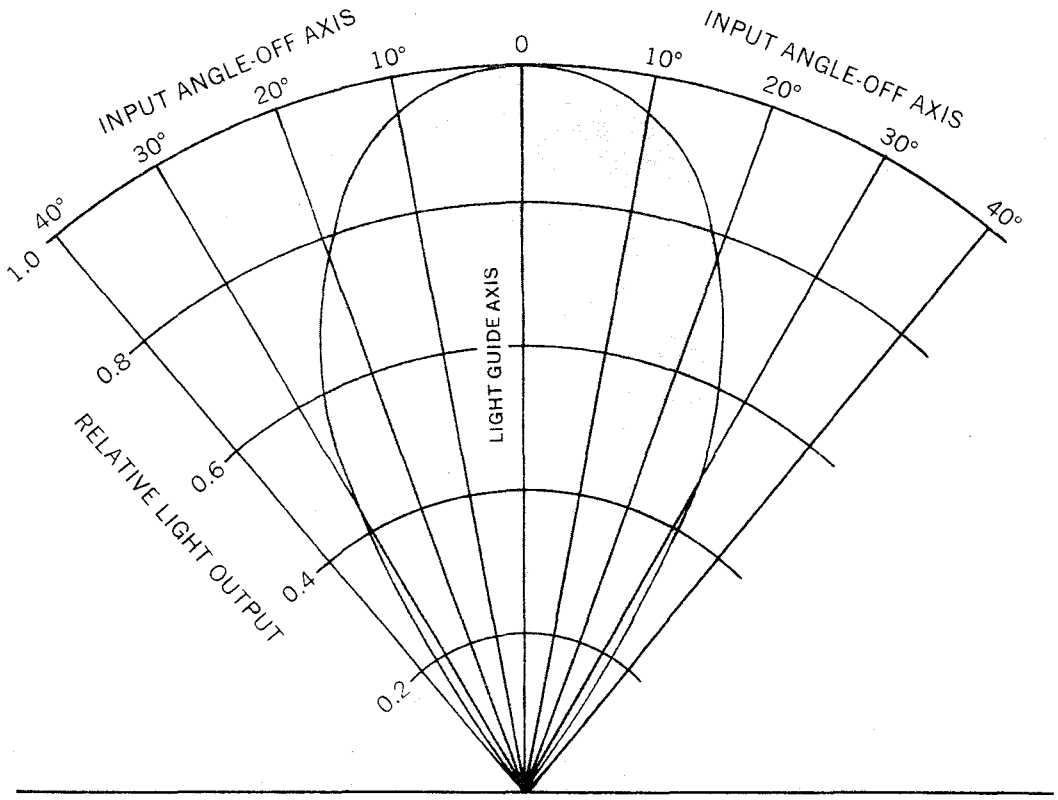

Fig. 22. Relative light output vs. input direction of collimated light for a fiber-optic probe.

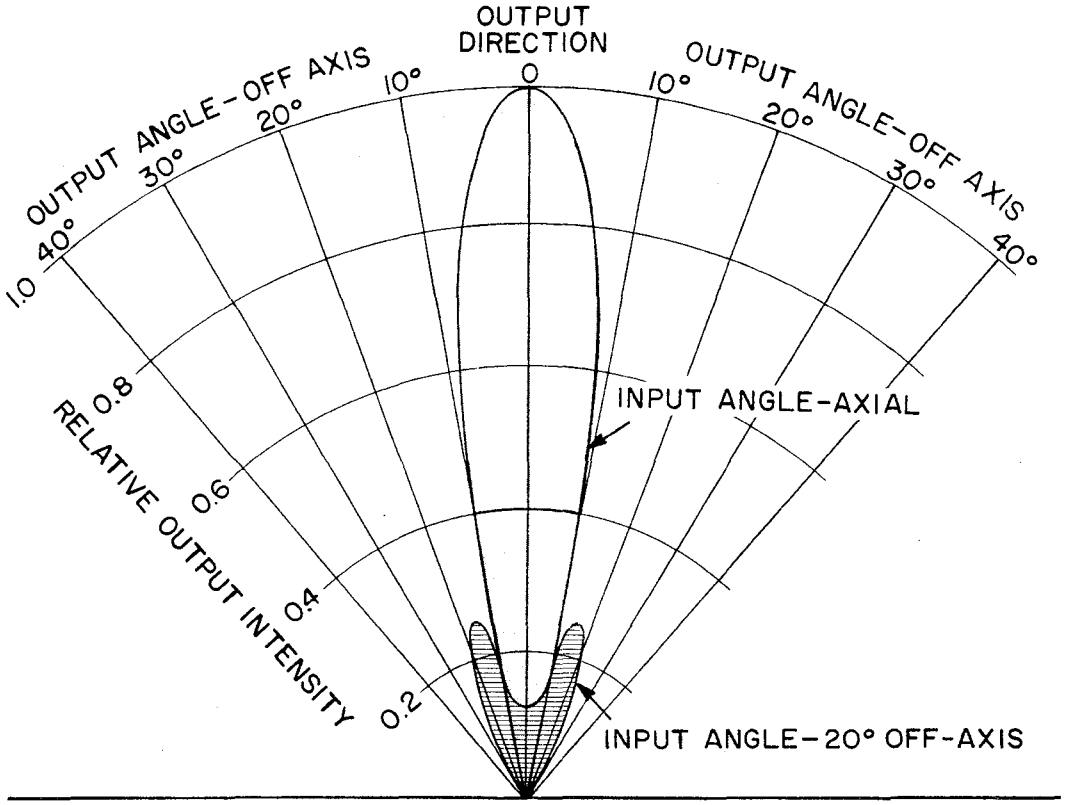

Fig. 23. Relative output intensity vs. output direction for a fiber-optic probe.

APPENDIX C

LITERATURE LISTING

Ament, W. S., "Toward a Theory of Reflection by a Rough Surface," *Proc. IRE*, 41:142, 1953.

Arsenault, H. H., "Roughness Determination with Laser Speckle," *J. Opt. Soc. Am.*, 61:1425-26, Oct., 1971.

Aughey, W. Henry and Baum, F. J., "Angular Dependence Light Scattering--A High Resolution Recording Instrument for the Angular Range 0.05 - 140°," *J. Opt. Soc. Am.*, 44:833-37, Nov., 1954.

Forward scatter measurements are made on particles in solution. Measurements are all made in the plane of the incident and transmitted light. Single wavelength measurements at mercury green were made over a dynamic range of 10^6.

Barkman, E. F., "Specular and Diffuse Reflecting Characteristics," Reynolds Metal Co., Metallurgical Res. Rept., 571-13A, April, 1959.

Barr, W. P., "Production of Low Scattering Dielectric Mirrors Using Rotating Vane Particle Filtration," *J. Sci. Instr.*, 2:1112-4, Dec., 1969.

Beaglehole, D. and Hunderi, O., "Study of the Interaction of Light with Rough Metal Surfaces," *Phys. Rev. B*, 2:309-29, July, 1970.

This paper described experimental results in the measurement of the reflectivity and scattering of microscopically rough surfaces. Measurements made confirm the good fit to the authors' theory. The theory is based on a random distribution of spheres on a surface. Plasmon effects as well as the additional fields from induced currents are discussed. Comparison is made to the results predicted by scalar theory. Measurements fall in the wide angle category.

Beck, J. W., "Multiple Beam Interferometry for Small Step Measurement," Nov., 1961, Stanford University, AD-273-455.

Beckmann, P., "Scattering by Composite Rough Surfaces," *Proc. IEEE*, 53:10-12-15, 1965.

Beckmann, P., "Scattering of Light by Rough Surfaces," Progress in Optics, Vol. VI, (E. Wolf, Editor), N. Holland Pub. Co., Amsterdam/London, 1968.

Beckmann, P., and Spizzichino, Andre, "The Scattering of Electromagnetic Waves from Rough Surfaces," Pergamon Press, Inc., New York, 1963.

Bennett, H. E., "Specular Reflectance of Aluminized Ground Glass and the Height Distribution of Surface Irregularities," *J. Opt. Soc. Am.*, 53:1389-94, Dec., 1963.

Early theory of specular reflectance as developed by Porteus and Bennett is applied to ground glass surfaces. It is shown that the height distribution of a surface may be found by taking the inverse Fourier transform of the square root of the coherent reflectance function. Wavelength vs. surface grind are plotted.

Bennett, H. E., "Measurement of Light Scattered from Very Smooth Surfaces," *J. Opt. Soc. Am.*, 60:1577, Nov., 1970.

The scalar theory as developed by Davies and Bennett and Porteus is reviewed. Instrumentation is described which measures light scattered between 1.5 and 20 degrees from the specular direction. Measurements are made with the light at normal incidence to the sample. Experimental technique is described in detail.

Bennett, H. E. and Koehler, W. F., "Precision Measurement of Absolute Specular Reflectance with Minimized Systematic Errors," *J. Opt. Soc. Am.*, 50:1-6, Jan., 1960.

Bennett, H. E. and Porteus, J. O., "Relation Between Surface Roughness and Specular Reflectance at Normal Incidence," *J. Opt. Soc. Am.*, 51:123-9, Feb., 1961.

(Abstract follows on next page.)

The roughness of a plane surface is related to its specular reflectance. Scalar theory is used and an expression for reflectance dependent upon the rms height of surface irregularities and the autocovariance length is derived following the work of Davies.

Bennett, J. M. and King, R. J., "Effect of Polishing Technique on the Roughness and Residual Surface Film on Fused Quartz Optical Flats," *Appl. Opt.*, 9:236-8, Jan., 1970.

Technique for producing and preparing extremely smooth optical surfaces is discussed. Ellipsometric methods are employed to measure surface films on samples that are highly polished.

Berreman, D. W., "Anomalous Reststrahl Structure from Slight Surface Roughness," *Phys. Rev.*, 163:855-64, March, 1967.

Birkebak, R. C. and Eckert, E. R. G., "Effects of Roughness of Metal Surfaces on Angular Distribution of Monochromatic Reflected Radiation," *J. Heat Trans.*, 87:85, 1965 (Ser. "C").

Describes a detailed experimental study to explore the influence of surface roughness conditions on the reflection characteristics of metal surfaces for nonthermal radiation. The test surfaces were prepared by standard optical grinding techniques using a range of grit sizes. Biangular, specular, and hemispherical-angular reflectance measurements are discussed in terms of the optical rms surface roughness, the wavelength of the reflected radiation, and the surface material. The results are compared with available predictions from theoretical analysis.

Blazey, Richard, "Light Scattering by Laser Mirrors," *Appl. Opt.*, 6:831-6, May, 1967.

Beckmann theory of scattering is applied to the particular case of dielectric laser mirrors. Wavelength dependent expressions are derived and qualitative experimental results are presented. The case of non-normal incidence is considered and measurements were made in this mode.

Born, M. and Wolf, E., Principles of Optics, Pergamon Press, Inc., 1959.

Brand, W. and Spagnolo, F. A., "Lambert Diffuse Reflection from General Quadric Surfaces," *J. Opt. Soc. Am.*, 57:452-8, April, 1967.

A general method for determining diffusely scattered light from quadric surfaces. The method assumes that the scattering objects are large and does not consider diffraction effects. Shadowing from concave surfaces is considered; multiple scattering is not. The theory should lend itself to the treatment of simple combinations of the basic geometries.

Brandenberg, W. M. and Neu, J. T., "Unidirectional Reflectance of Imperfectly Diffuse Surfaces," *J. Opt. Soc. Am.*, 56:97-103, Jan., 1966.

Brunsting, A. and Mullaney, P. F., "Light Scattering from Coated Spheres: A Model for Biological Cells," Rept. LA-DC 12883 from Los Alamos Scientific Laboratory, University of New Mexico.

Candidus, E. S. and Vanderschmidt, G. F., "Optical Surface Comparator," Paper presented at the Spring Meeting of the Optical Society of America, Abstract in *J. Opt. Soc. Am.*, 53:509.

Chenmoganadam, T. K., "On the Spectral Reflectance from Rough Surfaces," *Phys. Rev.*, 13:96, Jan., 1919.

Cheo, P. K. and Renan, J., "Wavelength Dependence of Total and Depolarized Back-Scattering of Laser Light from Rough Metal Surfaces," *J. Opt. Soc. Am.*, 59:821-6.

Christie, J. S., "An Instrument for the Geometric Attributes of Metallic Appearance," *Appl. Opt.*, 8:1777, Sept., 1969.

Coulson, K. L., "Effects of Reflection Properties of Natural Surfaces in Aerial Reconnaissance," *Appl. Opt.*, 5:905, June, 1966.

Croce, P., "On the Application of the Reciprocity Theorem to the Scattering Theory of Light," *Nouv. Rev. d'Optique Appliquée*, 3:249-52, 1972.

Dalmas, J., "Diffusion de la Lumière par une Demi-Sphère, Posée sur une Surface Plane, D'un Matériau de Même Nature," *Nouv. Rev. d'Optique Appliquée*, 1:167-70, Jan., 1970.

(Abstract follows on next page.)

Scattered light from a hemisphere on a plane surface of the same material is considered. One solution is arrived at by integrating the Helmholtz equation using a separation of variable technique. Employing the method of Twersky a good approximation to metallic surfaces can be made by assuming perfect conduction.

Dave, J. V. and Gazdag, J., "A Modified Fourier Transform Method for Multiple Scattering Calculations in a Plane Parallel Mie Atmosphere," *Appl. Opt.*, 9:1457, June, 1970.

Davies, H., "The Reflection of Electromagnetic Waves from a Rough Surface," *Proc. IEEE*, 101:209-14, July, 1954.

A "scalar scattering" theory is presented which considers just the phase modulation of the incident and outgoing light by the height variations along the surface. The resultant radiation distribution thus depends upon the phase of the wavelets, the phase of the incident field when it reaches a point on the surface. If the height variation is assumed gaussian with an rms deviation σ, this theory predicts the ratio of the specular reflectance of a smooth surface to vary as

$$\frac{R_\sigma}{R_o} \propto e^{-(4\pi\sigma/\lambda)^2}.$$

Similarly, predictions about the angular distribution of the scattered light are also made.

Depew, C. A. and Weir, R. D., "Surface Roughness Determination by the Measurement of Reflectance," *Appl. Opt.*, 10:969-70, April, 1970.

Experimental work done to determine the surface roughness of metals using reflectance measurements, and the Bennett and Porteus theory. Comparison with mechanical measurements is made. The results are said to substantiate the results of Bennett and Porteus.

Dietz, R. W. and Bennett, J. M., "Bond Tested Techniques for Producing Supersmooth Optical Surfaces," AD-644 340, Feb., 1966.

Dietz, R. W. and Bennett, J. M., "Bowl Feed Technique for Producing Supersmooth Optical Surfaces," Unclassified report from NOTS, China Lake, Feb., 1966, AD 644-340 (Report NOTS-TP-4224).

A method for producing very smooth surfaces on optical materials such as fused quartz or glass is described. The material being polished is kept immersed in a slurry of polishing compound and the final polishing is done with water containing no abrasive. Surfaces as smooth as 3A rms have been produced by this method.

Drude, P. and Danburg, Jerome, "Determination of the Optical Constants of Metals," AD-430 983.

Drummeter, L. F. and Fowler, W. B., "Angular-Reflectance Properties of Blackened Aluminum Honeycomb," Spring Meeting of the Optical Society of America, 1963.

Duffy, W., "A Simulation of the Effect of Sun Reflections from Chrome Surfaces on Visual Performance in a Variety of Viewing Situations," *Appl. Opt.*, 8:1803, Sept., 1969.

Egan, W. G., "Coherence-Polarization Phenomena in Remote Sensing," AD-849 398, March, 1969.

Einsport E., "Systematic Errors in the Determination of Optical Finish by Means of Fizeau Interference," AD-445 148, June, 1964.

Elson, J. M. and Ritchie, R. H., "Photon Interactions at a Rough Metal Surface," *Phys. Rev. B*, 4:4129, Dec., 1971.

The process of diffuse scattering and surface-plasmon creation by photons at a rough metal surface is discussed. A theoretical analysis employing quantum perturbation theory is used to calculate this scatter assuming a free electron model. Results that consider polarization are obtained and compared to those of Davies. The authors argue that their approach is better than that of Davies and that in fact his approach fails in the limit.

Endriz, J. G. and Spicer, W. E., "Study of Aluminum Films. I. Optical Studies of Reflectance Drops and Surface Oscillations on Controlled-Roughness Films," *Phys. Rev. B*, 4:4, Dec., 1971.

(Abstract follows on next page.)

Experiments are described that measure both plasmon-induced scattering and roughness-induced light scattering in aluminum films. In particular, the more recent theory of Elson and Ritchie is compared to results predicted by the scalar theory. Particular attention is paid to near UV wavelengths.

Estes, L. E., Narducci, L. M. and Tuft, R. A., "The Scattering of Light from a Rotating Ground Glass," Elec. Eng. Dept., Worcester Polytechnic Institute, 1971.

The statistics of a coherent light beam scattered by a rotating ground are investigated. The scattered light amplitude is confirmed to be a stochastic Gaussian variable. The scattered light power spectrum is shown to be a Gaussian function of the frequency. The experimental results agree very closely with theoretical predictions.

Felstead, E. B., "Additional Optical Data Processing Techniques for Surface Roughness Studies," *Proc. IEEE*, March, 1969, p. 344.

Finkel, M. W., "Integrating Sphere Theory," *Optics Communications*, 2:25, May/June, 1970.

Fischer, J. E., "Spurious Observations of Scattered Light in UV instruments," *Appl. Opt.*, 7:715-6, April, 1968.

Forbes, N., "Research on Laser Mirrors," AD-845 405, Nov., 1968.

Garbacz, R. J., "Electromagnetic Scattering from Radially Inhomogeneous Spheres," *Proc. IRE*, Aug., 1962.

The work of C. T. Tai is applied to electromagnetic scattering in radially inhomogeneous spheres. In particular equations are derived for computer use. The study applies to antenna theory.

Germogenova, O. A. and Siegel, A., "Intensity Fluctuations in Forward Scattering and Temporal Coherence," *Appl. Opt.*, 8:1849, Sept., 1969.

Forward scattering by a nonergodic system of identical particles is considered. The relation between the temporal correlation function of the scattered radiation and its second order

intensity moments is established. Estimates of this effect using infrared laser beam propagating through fog give results comparable to those of Tatarskii.

George, D. and Limperis, T., "Sources of Experimental Errors in Spectroscopic Measurements," AD-481 796, Jan., 1966.

Gloge, D., Chinnock, E. L., and Earl, H. E., "Scattering from Dielectric Mirrors," Bell Systems Tech J., 48:511-26, March, 1969.

The light scattered from high-reflecting dielectric mirrors is measured for angles between 0.01° to 1° from the beam axis over a wavelength range of 0.3 to 10 microns. A reasonable functional approximation for the measurements gives a scattered power density/sq. cm. at 0.1° of 10^{-6} of the total power (for 1.0 microns), and the power density varies inversely as the third power of the angle and the first power of the wavelength. For example, the power density would be 10^{-10} at 1.0° from a 10 micron beam.

Harrison, V. G. W., Definition and Measurement of Gloss, Parta, England, 1945.

Hass, G. and Hunter, W. R., "Laboratory Experiments to Study Surface Contamination and Degradation of Optical Surfaces in Simulated Space Environment," *Appl. Opt.*, 9:2101-10, Sept., 1970.

Hass, G. and Thum, R. E. (Editors), Physics of Thin Films, Vol. I-V, Academic Press, New York and London, 1966.

Hass, G. and Waylonis, J. E., "Optical Constants and Reflectance and Transmittance of Evaporated Aluminum in the Visible and Ultaviolet," *J. Opt. Soc. Am.*, 51:719-22, July, 1961.

Heinisch, R. P. and Jolliffe, C. L., "Light Baffle Attenuation Measurements in the Visible," *Appl. Opt.*, 10:2016-20, Sept., 1971.

Heinisch, R. P. and Schmidt, R. N., "Development and Application of an Instrument for the Measurement of Directional Emittance of Blackbody Cavities," *Appl. Opt.*, 9:1920, 1970.

Hensler, D. H., "Light Scattering from Fused Polycrystalline Aluminum Oxide Surfaces," *Appl. Opt.*, 11:2522-28, Nov., 1972.

Hodgkinson, L. J., "Optical Flat Surface Roughness," *Brit, J. Sci. Inst.*, 3:300-4, April, 1970.

Holl, H. B., "Specular Reflection and Characteristics of Reflected Light," *J. Opt. Soc. Am.*, 57:1967-90, May, 1967.

Hostletter, G. R., "Measurement of Scattered Light from Mirrors and Lenses," *Appl. Opt.*, 7:1383-5, July, 1968.

Hulst, H. D. van de, Light Scattering by Small Particles, Wiley, New York, 1957.

Hunter, R. S., "A Multipurpose Photoelectric Reflectometer," *J. Opt. Soc. Am.*, 36:536-59, Nov., 1940.

A reflectometer is described that was used to measure glass, bloom, specular gloss, sheen and luminous apparent reflectance. All but the specular glass measurements are measures of scattered light. Samples were primarily porcelain enamels. This is one of the earliest papers where a photoelectric tube was used to measure scatter.

Hunter, R. S., "A New Goniophotometer," Proceedings of the Optical Society of America, circa 1950.

Hunter, W. R., "Errors in Using the Reflectance vs. Angle of Incidence Method for Measuring Optical Constants," *J. Opt. Soc. Am.*, 55:1197, Oct., 1965.

Hunter, W. R., "On the Cause of Errors in Reflectance vs. Angle of Incidence Measurements and the Design of Reflectometers to Eliminate the Errors," *Appl. Opt.*, 6:2140, Dec., 1967.

The accuracy of reflectance measurements is discussed. Calibrating techniques, alignment, nonuniform illumination, detector response, linearity, stray light, and source fluctuations are all discussed as ways to minimize the effect of these factors.

Johnson, M. C., "Vacuum Ultraviolet Scattering Distributions," *Appl. Opt.*, 7:879-81, May, 1968.

Johnston, R. G., Canfield, L. R., and Madden, R. P., "Reflective Scattering from Substrates and Evaporated Films in the Far Ultraviolet," *Appl. Opt.*, 6:719-22, April, 1967.

The bi-directional reflectance of mirror surfaces in the far UV are reported. Aluminum and Gold films are both considered. Results indicate best

results from fused silica substrates. Radiation is measured beyond 10° only. The theory of Bennett and Porteus is used.

Johnston, R. G. and Madden, R. P., "On the Use of Thermopiles for Absolute Radiometry in the Far Ultraviolet," *Appl. Opt.*, 4:1574, Dec., 1965.

In particular the scattering properties of gold-black are measured in the far UV. A goniphotometer is used for these measurements. Other aspects of radiometry in the UV are also discussed.

Jones, L. A., "The Gloss Characteristics of Photographic Papers," *J. Opt. Soc. Am.*, 6, 140(1922).

Judd, D. B., "Terms, Definitions, and Symbols in Reflectometry," *J. Opt. Soc. Am.*, 57:445-452, April, 1967.

A clear notation for reflectometry is set forth. Examples, diagrams, and mathematical models help clarify the definitions.

Keegan, H. J. and Weidner, V. R., "Infrared Spectral Reflectance of Black Materials," Paper presented at 1966 Annual Meeting of the Optical Society, Abstract in *J. Opt. Soc. Am.*, 56:1453.

Kelsall, D., "Absolute Specular Reflection Measurements of Highly Reflecting Optical Coatings at 10.6 Microns," *Appl. Opt.*, 9:85-90, Jan., 1970.

Kerker, M., The Scattering of Light and Other Electromagnetic Radiation, Academic Press, New York, p. 666, 1969.

A recent text that estensively covers the subject of electromagnetic scattering, particularly that of light scattering. Emphasis is on scattering from particles or on passage through a nonhomogeneous media rather than from surfaces.

Kerker, M., "A Light Scattering of Monodispersed Polystyrene Latexes," AD-231 625.

Koehler, W. F. and Eberstein, A., "Surface Topography and Optical Properties of Multilayer Films," AD-90 627.

Koehler, W. F. and White, W. C., "Multiple-Beam Fringes of Equal Chromatic Order, Part VI Method of Measuring Roughness," *J. Opt. Soc. Am.*, 45:1011, 1955.

Kovar, N. S., Kovar, R. P., and Bonnen, G. P., "Light Scattering by Manned Spacecraft Atmospheres," *Planet and Space Sci.*, 17:143-54, Feb., 1969.

Lavin, E. P., Monographs on Applied Optics No. 2, Specular Reflection, American Elsevier Publishing Co., Inc., New York, 1971.

Longuet-Higgins, M. S., "Reflection and Refraction at a Random Moving Surface. I. Pattern and Paths of Specular Points, II. Number of Specular Points in a Gaussian Surface, III. Frequency of Twinkling in a Gaussian Surface," *J. Opt. Soc. Am.*, 50:838-51, Sept., 1960.

Look, D. C. J. R., "Diffuse Reflection from a Plane Surface," *J. Opt. Soc. Am.*, 55:1628-32, Dec., 1965.

Measurements are described that determine the angular dependence of the amount of radiation scattered from plane diffuse surfaces; the results have peak levels of as much as 10% from those predicted by the use of Lambert's law of diffuse reflection. An empirical expression is derived that agrees with the measured results within 2%. The expression is believed to hold good for any diffuse reflective surface (a surface that has no large specular component of reflection).

Lotsch, H. K., "Reflection and Refraction of a Beam of Light at a Plane Interface," *J. Opt. Soc. Am.*, 58:551-61, April, 1968.

Maltby, P., "The Effect of Scattered Light on Solar Intensity Observations as Derived 9 May 1970 Mercury Transit," *Solar Physics*, 18:3-21, May, 1971.

Marathay, A. S., Heiko, L., and Zuckerman, J. L., "Study of Rough Surfaces by Light Scattering," *Appl. Opt.*, 9:2470-76, Nov., 1970.

The scattered field is examined in order to derive the intrinsic properties of a moving rough surface. The formulation is cast in the framework of scalar coherence theory. It is shown that the statistical properties of the scattered field are affected much more by the media that introduce random phase than by those that introduce random amplitude absorption.

Middleton, W. E. K. and Wyszecki, G., "Colors Produced by Reflection at Grazing Incidence from Rough Surfaces," *J. Opt. Soc. Am.*, 47:1020, Nov., 1957.

Specular reflection from optically rough surfaces is investigated at large angles. The dependence of the specular reflection on wavelength is noted for the case of ground glass surfaces.

Mitzner, Kenneth M., "Theory of the Scattering of Electromagnetic Waves by Irregular Interfaces," Cal. Tech. Antenna Lab. Report TR30, Jan., 1964.

Problems involving electromagnetic scattering from irregular interfaces are treated. Both deterministic and statistical irregularities are considered. Interfaces with both large irregularities and small irregularities are treated. Matrix transformations are utilized to obtain rather complex solutions.

Moffat, D. L., "A Physical Optics Approximation of the Scattering for Axial Incidence from Rotationally Symmetric Targets," AD-256 329.

Möller, F., "Optics of the Lower Atmosphere," *Appl. Opt.*, 3:157, Feb., 1964.

Mott, L. P., "The Effect of Surface Roughness on the Optical Properties of All-Dielectric Interference Filters," MS Thesis, U. of Ariz., 1971.

McCamy, C. S., "Concepts, Terminology, and Notation for Optical Modulation," *Photographic Sci. and Eng.*, 10:314, Nov.-Dec., 1966.

A system for describing transmittance, reflectance, and absorptance in photography is described. This article can be regarded as a companion article to that of Judd reference above in this bibliography.

McKenney, D. B., Orme, G. R., and Mott, L. P., Light Scattering by Thin Film Coatings, Optical Sciences Center, U. of Arizona, Jan., 1972.

McNicholas, H. J., "Absolute Methods in Reflectometry," *Bur. Std. J. Res.*, 1:29-73, Jan., 1928.

(Abstract follows on next page.)

Theory of the integrating sphere is presented. Relationships between specular and diffuse illumination are derived and applied. Both relative and absolute methods are discussed in the measurement of reflectance.

Nagaraja Reo, C. R., Chen, H. S., and Takashima, T., "Laboratory Determination of the Characteristic Reflection Matrices of Natural Surfaces," *Brit, J. Appl. Phys.*, (D) 4:1057-62, July, 1971.

Nelson, H. F., and Gouland, R., "Reflection from a Periodic Dielectric Surface," *J. Opt. Soc. Am.*, 57:769-71, June, 1967.

Newkirk, Jr., Gordon, and Bohlin, David, "Reduction of Scattered Light in the Coronagraph," *Appl. Opt.*, 2:131-40, Feb., 1963.

The use of apodized discs (baffling) is used to reduce scattered light in coronagraphs. Surface properties of reflecting optics are mentioned only qualitatively.

Nicholls, R. L., "Near Infrared Diffuse Reflectivities of Natural and Manmade Materials," *Brit. J. Appl. Phys.*, (D) 2:201-4, Feb., 1969.

Nicodemus, F. E., "Directional Reflectance and Emissivity of an Opaque Surface," *Appl. Opt.*, 4:767-73, July, 1965.

Terminology, concepts, and symbols relating to the directional reflectance of an opaque surface. Integral relationships are related to the measured data.

Nicodemus, F. E., "Reflectance Nomenclature and Directional Reflectance and Emissivity," *Appl. Opt.*, 9:1474-5, July, 1970.

O'Brien, P. F., "Directional Reflectances of Room Surfaces," *Illum. Eng.*, 64:245-52, April, 1969.

Ohlidal, I., Navratil, K., and Lukes, F., "Reflection of Light by a System of Nonabsorbing Isotropic Substrate with Randomly Rough Boundaries," *J. Opt. Soc. Am.*, 61:1630-39, Dec., 1971.

Ohlidal, I., Navratil, K., and Lukes, F., "Reflection of Light on a System of Non-Absorbing Isotropic Film--Non-Absorbing Isotropic Substrate with Rough Boundaries," *Optics Communications*, 3:40, March, 1971.

(Abstract follows on next page.)

A scalar approach to the reflection of light from a thin film coating is considered. The Kirchhoff conditions are assumed. Two cases are considered: the first is that of identical boundaries on both sides of the film and the second that of independent boundaries. Experimental results are given that agree with the identical thin film model.

Orme, G. R., "Measurement of Saml1 Angle Scatter from Smooth Surfaces," Tech. Rept. 74, Optical Sciences Center, U. of Arizona, 1972.

Porteus, J. O., "Relation between the Height Distribution of a Rough Surface and the Reflectance at Normal Incidence," *J. Opt. Soc. Am.*, 53:1394-1402, Dec., 1963.

Progelhof, R. C. and Throne, J. L., "Radiation Characteristics of a Scattering, Absorbing Dielectric Sheet," *Appl. Opt.*, 9:2359-61, Oct., 1970.

The two flux method of Klien, Progelhof and Throne is analyzed using knowledge of the relationship between internal and external reflectance. Order of magnitude solutions are arrived at. A more sophisticated method is suggested.

Ranbauske, W. R., and Gruenzel, R. R., "Distribution of Diffuse Optical Reflection Around Some Sterometric Surfaces," *J. Opt. Soc. Am.*, 55:315-18, March, 1965.

Ratcliffe, J. A., "Some Aspects of Diffraction Theory and Their Application to the Ionosphere," Reports on Progress in Physics, Vol. XIX, (1956), The Physical Society, London.

Rayleigh (Right Hon. Lord, F. R. S.), 1901, "Polish," *Nature*, 64:385-388.

Rennilson, J. J., Holt, H. E., and Morris, E. C., "Measurements of the Photometric Properties of an Area on the Lunar Surface," *J. Opt. Soc. Am.*, 58:747, June, 1968.

Rice, S. O., "Reflection of Electromagnetic Waves from Slightly Rough Surfaces," Symposium of the Theory of Electromagnetic Waves (Interscience Publishers, New York, 1951), p. 351.

Rigden, J. D., and Gordon, E. I., "The Granularity of Scattered Optical Maser Light," *Proc. IRE*, Nov., 1962.

The granular nature of scattered laser light is described and explained.

Ross, W. D., "Computation of Bessel Functions in Light Scattering Studies," *Appl. Opt.*, 11:1919-23, Sept., 1972.

Ruze, John, "Antenna Tolerance Theory--A Review," AD-642 205, Lincoln Lab., Massachusetts Inst. of Tech., Lexington, Mass., Dec., 1965.

The theoretical basis of antenna tolerance theory is reviewed. Formulas are presented for the axial loss of gain and the pattern degradation as a function of the reflector surface rms error and the surface spatial correlation.

Sawatari, T., "Surface Flaw Detection Using Oblique Angle Illumination," *Appl. Opt.*, 11:1337-44, June, 1972.

A method for detecting surface flaws using oblique angle illumination. The effect of various surface finishes is considered. The relation between surface roughness and the diffraction pattern is given as a function of the angle of incidence in the illuminating beam and the feasibility for flaw detection is discussed.

Semplak, R. A., "0.63 Micron Scatter Measurements from Teflon and Various Metallic Surfaces," Bell Systems Tech. J., Oct., 1965, pp. 1659-74.

The angular dependence of several teflon and metallic surfaces are measured. A method for measuring scatter close to the spectral direction is also given. Several models are introduced to explain the various scatter profiles measured. Data obtained is also numerically integrated to obtain total scatter information.

Shaw, J. E., and Blevin, W. R., "Instrument for the Absolute Measurement of Direct Spectral Reflectances at Normal Incidence," *J. Opt. Soc. Am.*, 54:334-6, March, 1964.

Shipley, E. N., "Multiple Scattering Calculations--Geometry for Spherical Atmospheres," Bellcom, Inc., Wash., D. C., 16 April 1971, NASA-CR-118662 TM-71-1011-5.

Singh, K., and Bhatnagar, G. S., "Sparrow Limit of Spectral Resolution in the Reflection Echelon and the Fabry-Perot Interferometer Having Surface Imperfections," *Appl. Opt.*, 9:2326, Oct., 1970.

Slater, J. M., "A Recording Goniophotometer," *J. Opt. Soc. Am.*, 21:218-23, July, 1935.

Spagnolo, F. A., "Lambert Scattering from an Elliptic Cylinder," *Appl. Opt.*, 11:2890-93, 1972.

Spartan, T. M., "Scattering of Coherent Light from a Rough Surface," *Brit. J. Appl. Phys.*, 2:1027-34, July, 1969.

Starner, K., "Effects of Front Surface Roughening on Solar Absorptivity of Quartz Rear Surface Mirror Satellite Coatings," AD-815 036.

An experimental investigation was conducted to determine the possible increase of the solar absorptivity of quartz rear surface silvered mirrors due to surface roughness effects. Close agreement between data and analytical model results were obtained. It is postulated that absorptivity increase is caused by surface scattering of incoming and reflected radiation. Such scattering gives rise to total multiple reflections within the quartz layer due to the critical angle effects.

Tobin, R. C., "Rayleigh Scattering from Defects in Quartz," *Appl. Opt.*, 8:1855, Sept., 1969.

Todd, E. P., "Specular Reflection from a Spherical Surface," Upper Air Laboratory, Physics Department, U. of Colorado, *J. Opt. Soc. Am.*, May, 1959.

Torrence, K. E., "Monochromatic Directional Distribution of Reflected Thermal Radiation from Roughened Dielectric Surfaces," MS Thesis, U. of Minnesota, 1964.

Twersky, V., "Reflection Coefficients for Certain Rough Surfaces," *J. Appl. Phys.*, 24:629-60, May, 1953.

Twersky, V., "On Scattering and Reflection of Electromagnetic Waves by Rough Surfaces," *IRE Transactions on Antennas and Propagation*, pp. 81-90, Jan., 1957.

White, John U., "New Method for Measuring Diffuse Reflectance in the Infrared," *J. Opt. Soc. Am.*, 54:1332-37, Nov., 1964.

Wood, B. E., "Vacuum Integrating Spheres for Measuring Cryodeposit Reflectances from 0.35 to 15 Microns," Arnold Eng. Ctr., Arnold Air Force Station, Rept. No. AEDC-TR-65-176, AD-468 609, Aug., 1965.

Woodman, T. P., "Light Scattering in Porous Anodic Aluminum Oxide Films I. Colour Effects, II. Polarization Effects," *Thin Solid Films*, 9, 1972, pp. 195-389.

Wolf, E., "Generalized Fourier Techniques for the Theory of Light Scattering," Final Report, 1 Jan. to 31 Dec., 1970, Rochester U., New York, Dept. of Physics and Astronomy, Jan., 1971, AD-720858, AFCRL-71-0114.

Young, R. D., "Surface Microtopography," *Phys. Today*, p. 42, Nov., 1971.

Zipin, R. B., "A Preliminary Investigation of the Bidirectional Spectral Reflectance of V-Grooved Surfaces," *Appl. Opt.*, 5:1954, Dec., 1966.

REPORT DISTRIBUTION LIST

SAMSO (DYAX)
AF Unit Post Office
Los Angeles, California 90045 (15 copies)

Defense Documentation Center (DDC)
Cameron Station
Alexandria, Virginia 22314 (12 copies)

Air University Library
Maxwell AFB, Alabama 36112 (1 copy)